

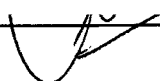
AN ABSTRACT OF THE THESIS OF

Abdulahdi M. Alajmi for the degree of Master of Science in Electrical and Computer Engineering presented on October 29, 1993.

Title : Design Procedure for Brushless Doubly-Fed Machine used as a Limited Speed-Range Pump Drive

Redacted for privacy

Abstract approved :



Alan K. Wallace

The continuing desire of industry to further improve process efficiency, through tighter control and energy conservation, has prompted users to pay closer attention to Adjustable Speed Drives (ASDs). The conventional ASDs consist of induction or synchronous motors controlled by power electronic controllers through the adjustment of supply frequency and line voltage. The drawback of these conventional ASDs lies in the high cost of the power electronic controllers which have the same rating as that of the machine itself.

The Brushless Doubly-Fed Machine (BDFM) ASD has proven, both analytically and experimentally, to provide a cost effective and a wide range of precise speed control. The experimental BDFM prototypes built to date were designed and constructed individually based on designers' experience with self-cascaded machines. The success with these prototypes has promoted the idea of standardizing the design procedure for all future BDFMs. This thesis offers a general design procedure for the BDFM, which can serve as a first step in standardizing the manufacturing process of this machine. The procedure is presented in the form of a demonstration, by applying it to the design of a 60-hp, 600 to 900 r/min, 460-volts BDFM pump drive to replace the currently utilized

conventional 60-hp wound rotor induction motor ASD. An ideal design, which determines machine details such as physical dimensions, slot specifics and conductor details based on conservative magnetic and electric loading assumptions, is one form of the design procedure. The other form, the practical design, involves utilizing a specified physical dimensions and slot details to determine the associated conductors' details and to insure the compliance of machine loadings with up-to-date industrial standards. In both procedures, the design will be made to satisfy, if not to exceed, the existing conventional drive performance.

© Copyright by Abdulhadi Alajmi

October 29, 1993

All Rights Reserved

**DESIGN PROCEDURE FOR
BRUSHLESS DOUBLY-FED MACHINE
USED AS A
LIMITED SPEED - RANGE PUMP DRIVE**

by

Abdulahdi M. Alajmi

A THESIS

submitted to

Oregon State University

in partial fulfillment of

the requirement for the

degree of

Master of Science

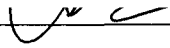
Completed October 29, 1993

Commencement June 1994

APPROVED:

Redacted for privacy

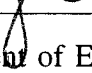
November 12th 1993



Professor of Electrical and Computer Engineering in Charge of Major

Redacted for privacy

Nov. 12, 1993



Head of Department of Electrical and Computer Engineering

Redacted for privacy

Dean of Graduate School

Date thesis is presented October 29, 1993

Typed by Hadi Alajmi

DEDICATION

To Aramco I dedicate this work.

ACKNOWLEDGEMENTS

I would like to express my thanks and gratitude to my company, Saudi Aramco, for sponsoring my college and Master program education. In particular, I would like to thank my department, Consulting Services, for offering me the opportunity and expressing their confidence in me to continue my higher education. I hope to fulfill if not to exceed the expectations set for this assignment. Thanks are due to my managements, R.V.Boyd, Aziz Ashban, Pip Reah for their understanding and cooperation and for being very helpful during the tough days prior to the commencement of the assignment. Special thanks and appreciations to Rienk Tuin for his continuous support and his invaluable guidance and advice before and during the course of this assignment. I would like to thank Troy Mallory for his recommendations to begin and encouragement to continue my higher education program.

I gratefully thank my major professor, Alan K. Wallace, for his support and proper guidance and for his insistence on me to continue the thesis option. This is truly an invaluable experience and undoubtedly is a major step toward specializing in this field. His advice and encouragement in crucial times are critical to the completion of this thesis in particular and the program in general. Thanks are also due to professor René Speé for providing the data acquisition system, for reviewing the design and giving his positive suggestions. Sincere thanks to Art Neely for the time and effort he gave to prepare the data acquisition system used for this project.

Thanks are also due to Dan Hanthorn, Dave Zinda, Kirby.... and the rest of Corvallis Waste Water Treatment Plant personnel for their assistance and for making my activity at their plant more convenient.

Finally my thanks are undoubtedly due to my wife and two children for their patience, understanding and support during these crucial two years of our lives. I am sorry for the lack of time given to them and I promise them better days ahead.

TABLE OF CONTENTS

1. Introduction	1
2. Existing System Study	4
2.1 Process Overview	4
2.2 ASD Justification	6
3. Existing Drive Performance Analysis	7
3.1 Tests Performed	7
3.2 Test Setup	8
3.3 Analysis	9
4. Design of Brushless Doubly Fed Machine	15
4.1 Background	15
4.2 BDFM Design Procedure Overview	17
4.3 Machine and Winding Ratings	18
4.4 Six Pole Winding Design	26
4.4.1 Magnetic and Electric Loadings (B_g, Q)	27
4.4.2 Stator Slot Calculations	30
4.4.3 Winding Factor (d)	32
4.4.4 The Physical Volume of The Machine ($D^2 * L_a$)	33
4.4.5 Diameter and Axial Length Determination (D, L_a)	37
4.4.6 Number of Conductors Calculations (C_s, Z)	38
4.4.7 Slot and Tooth Width Determination	39
4.4.8 Conductors Sizes and Numbers	42
4.4.9 Required Slot Depth	43

4.4.10 Number of Turns and Winding Resistance	44
4.4.11 Winding Resistance and Copper Loss	45
4.4.12 Core Flux Density and Depth	48
4.4.13 6-Pole Winding Iron Loss	49
4.5 Two-Pole Winding Design	51
4.6 Common Calculation For Both Windings	52
4.7 BDFM Rotor Design	54
4.7.1 Preliminary Calculations	55
4.7.2 Rotor Bar Currents and Sizes	57
4.7.3 Slot and Teeth Width	59
4.7.4 Rotor Resistances and Copper losses	60
4.7.5 Flux profile and Iron losses	62
4.7.6 Calculated efficiency	63
4.8 Practical Design	63
4.9 Design Sheets and Their Layouts	65
5. Conclusion and Recommendation	67
6. Bibliography	69
Appendix-I; Pump Station Flow Chart, Irregular Flow	71
Appendix-II; Pump Station Flow Chart, Steady Flow	72
Appendix-III; Raw Data Averaging Sample	73
Appendix-IV; Collection of All Raw Data Averages, Stator	74
Appendix-V; Collection of All Raw Data Averages, Rotor	75
Appendix-VI; Existing Drive Performance Analysis Table	76

Appendix-VII; Slot Combination Table	77
Appendix-VIII; Winding Layout and Corresponding MMF Waveform, 6-Pole	78
Appendix-IX; Winding Layout and Corresponding MMF Waveform, 2-Pole	79
Appendix-X; BDFM Ideal Design Spreadsheet	80
Appendix-XI; BDFM Practical Design Spreadsheet	98

LIST OF FIGURES

<u>Figure</u>	<u>Page</u>
Figure 2.1 Pump station load duty cycle (1-month period)	5
Figure 2.2 Pump station load duty cycle (6-month period)	6
Figure 3.1 Existing drive test set-up	8
Figure 3.2 Per phase equivalent circuit and associated measurements	10
Figure 3.3 Drive power flow diagram	11
Figure 3.4 Existing drive input/output power	13
Figure 3.5 Existing drive external resistor losses	13
Figure 3.6 Existing drive and pump performance	14
Figure 3.7 Existing drive performance	14
Figure 4.1 Brushless doubly fed machine (BDFM) drive	17
Figure 4.2 BDFM- frequency and speed schedule	24
Figure 4.3 Power factor variation of 3-phase induction motor (at 100% rated load)	26
Figure 4.4 Efficiency variation of 3-phase induction motor (at 100% rated load)	27
Figure 4.5 Electric loading of air-gap periphery of induction motor	30
Figure 4.6 Slot and tooth layout	44
Figure 4.7 Winding length schematics	45
Figure 4.8 Polyphase machine flux path	48
Figure 4.9 Iron losses per pound	50
Figure 4.10 BDFM flux waves interactions	53
Figure 4.11 BDFM rotor structures	55
Figure 4.12 Rotor nest currents distribution	58
Figure 4.13 Rotor slot and tooth configuration	59
Figure 4.14 Slot area equivalent	65
Figure 4.15 Design spreadsheets layouts	66

LIST OF TABLES

Table 4.1	BDFM windings rating	25
Table 4.2	Equivalent induction machine winding ratings	25

DESIGN PROCEDURE FOR
BRUSHLESS DOUBLY-FED MACHINE
USED AS A
LIMITED SPEED-RANGE PUMP DRIVE

1. Introduction

Adjustable Speed Drives (ASD) popularity is increasing rapidly due to pressure from industry for more efficient and reliable drive systems and the ever increasing advancements and confidence in power electronic controllers and their capabilities. In the past, the drawbacks of such drives were primarily due to the high capital cost associated with the power electronic controllers which limited the payback to investments in such drives [1]. Therefore, ASDs were only employed in critical processes and their popularity was limited. However, the advancements in power electronics in recent years has made it possible for manufacturers to provide the market with ranges of highly reliable and less expensive controllers [2]. This in turn, along with the world awareness to conserve energy, has prompted industry to renew their interest in such valuable alternatives.

In industry, ASDs find most applications in pumps, compressors and fans, where normally process operation requirements were met through the employment of recycling valves and dampers. Such means of control are not only an additional capital investment and source of maintenance trouble, but most importantly a waste of limited energy resources. A typical ASD consists of a conventional induction or synchronous motor controlled by varying the supply frequency and voltage to attain the desired speed. As a result, the controller rating must at least be the same full load rating as the machine itself. This causes the cost of the controllers to increase significantly, especially in applications where high power drives are required. Other concerns

involve the high harmonic contents, associated with the currents drawn by these power converters, which pollute utility's lines or which require investments in harmonic filters in order to comply with the newly established IEEE Standard 519 [1,2,3].

The above economical and reliability concerns has prompted the ECE Energy Systems group at OSU to investigate both the ASD and Variable Speed Generator (VSG) since early 1980s [1]. The Brushless Doubly Fed Machine (BDFM), where self-cascading induction motors incorporated in one frame are employed, was the result of these investigations [1,2,3]. Since then, proof of concept prototypes were designed and tested over a wide speed range in both motoring and generation modes and by using conventional Pulse Width Modulation (PWM) and an experimental Series Resonant (SR) converter [1]. These experimental prototypes have demonstrated several advantages over conventional ASDs.

In contrast to conventional ASDs, the converter rating was shown analytically and experimentally to be a fraction of the machine rating depending upon the particular application speed range. This not only offers a low capital investment in controllers but also reduces, if not eliminates, the harmonic content returned to the supply line through the adjustment of the control winding excitation. Further, it was shown that this machine offers a more precise control over a wide speed range and a high system availability due to flexibility in operating as a regular induction motor in the event of controller failure [1].

Three phases, out of a possible four phase program, in the research and development of BDFM, have been completed with promising success. In the first Phase, technical feasibility, machine modeling and operation predictions were the focus of the study [1,4,5]. The encouraging results were then capitalized upon in Phase Two by emphasizing improvement in machine design, speed range and control strategy [6].

Phase Three of this program involved the optimization of construction techniques of the lab prototypes and paved the way for an industrial application prototype in Phase Four [6,7].

The continual success in the analysis and the proof of concept designs of this machine through Phase Three has increased the confidence in BDFM capabilities to be a valuable alternative as conventional ASDs. This confidence has prompted OSU faculty and Corvallis Waste-Water Treatment Plant (CWWTP) operations personnel to consider the replacement of the current 60-HP Wound-Rotor Induction Machine (WRIM) ASD drive with an equivalent BDFM drive. In the current drive, speed control is achieved via external resistors where energy is dissipated as heat. From several available alternatives, BDFM was selected for trial installation because of the advantages, discussed above, it offers in this application.

This thesis will present a detailed design procedure for the BDFM in general and for this application in particular. The design will be based on the design procedure for induction machines, but keeping in mind the unique stator and rotor structure of the BDFM. The design will be carried out by means of spreadsheets, which allow for variable adjustments and future modification to suit any future designs. For the purpose of this project, a study of this particular application and an investigation of the existing drive performance will also be presented. This will help set up the performance requirements for the BDFM.

2. Existing System Study

2.1 Process Overview

The Corvallis Waste Water Treatment Plant (CWWT) includes an influent pump station which is required to lift the influent fluid from wet well level to plant level 37 ft higher. Four pumps are utilized for this application, three of which are rated @ 125 HP with capacity of 14 Million Gallon Per Day (MGPD) each and one is rated @ 60 HP with capacity of 7 MGPD. The four pumps are commonly know as P-2211, P-2212, P-2213, P-2214 with the 60 HP as P-2213. This project is concerned with the drive to the smaller pump, P-2213.

P-2213 has the lowest rating of all the pumps with capacity of 7 MGPD which make it a good candidate for being used as the follow pump in the sequence during peak operation periods (wet season). However, in the dry season it is generally used as the follow pump only during peak hours and as the main pump running during non-peak hours. In the latter application, the pump drive is almost always operating at its full load speed 870-rpm, even though the pump capacity is not yet reached. These periods usually occur when the wet well level increases beyond the speed capability of the drive, thus mandating another pump to be turned on for a short period of time to fulfill the well's level increase requirements. This causes a cyclic switch-on and switch-off of the follow pump and leads to an irregular operation pattern. Two plant flow charts are attached in Appendices-I and II which demonstrate the severe irregularities in plant flow due to the above operation sequences and a desired steady plant flow respectively.

When the small pump is used as the last follow pump in the sequence, it is always in the variable speed mode. However, as will be shown in Chapter 3, the drive performance at too low speed is unstable, which in turn minimizes the speed range of operation and causes an irregular plant operation, as discussed above.

P-2213 is driven by a 60-Hp, 3-phase, 460-volts, 60-Hz, 8-pole, 900-r/min wound rotor induction motor. The designed speed range is 600 to 870 r/min and speed control is accomplished by varying the rotor external resistors. It was not possible to determine this particular drive's load duty cycle alone as was anticipated, due to the lack of individual pump flow meters. The only flow meter available is installed on the main header and records plant total flow. However, from this flow data it was possible to obtain the pump station load duty cycle which is an indication of the individual pumps' duty cycles. Two load duty cycle graphs are presented here. The first one corresponds to flow data obtained for the month of January 1993. The second graph correspond to flow data, obtained from plant records, for a six month period of the previous year.

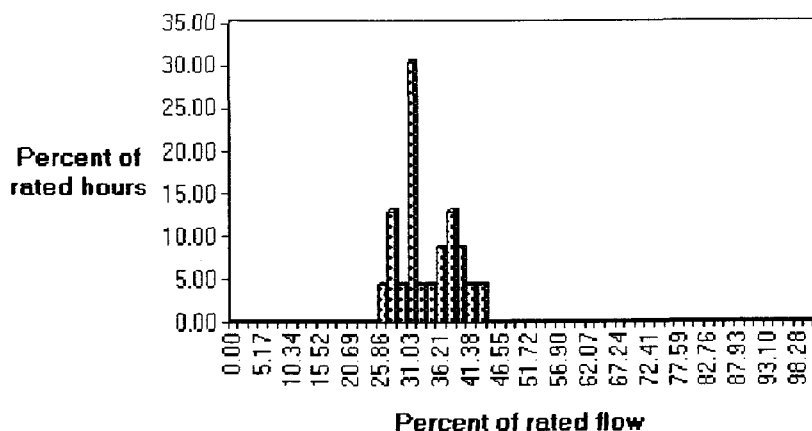


Figure 2.1 Pump station load duty cycle (1-month period)

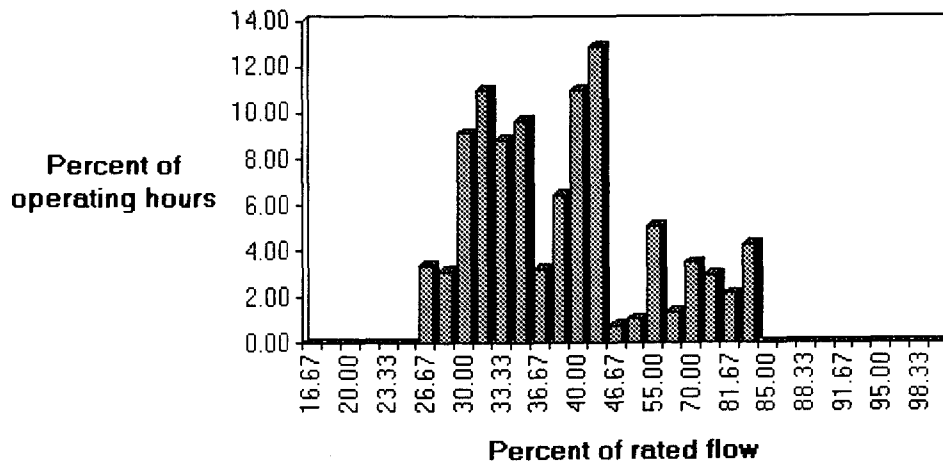


Figure 2.2 Pump station load duty cycle (6-month period)

2.2 ASD Justification

From the above two graphs and the flow charts in Appendix I and II, it is evident that the pump drives are required to operate for very significant periods at lower than their rated top speed and output power. Hence, an ASD is justified in this application and, in particular, it can be concluded that this drive is suitable to a precise speed control which we believe can be achieved by the employment of BDFM adjustable speed drive. In addition, operation personnel have expressed their preference to increase the upper speed limit from 870 to 900 rpm, a criteria which can be accomplished readily by the BDFM.

3. Existing Drive Performance Analysis

3.1 Tests Performed

To insure that the performance of the proposed BDFM drive satisfies the current and future operation requirements, the performance of the existing drive was investigated. Two tests were conducted on this drive in order to characterize its performance. The first test consisted of collecting data from the machine every minute for a 30 minute period. This test was conducted while the drive was operating in parallel with another one. Plant operational personnel expressed concerns that the small drive might not be able to handle the complete requirements at that time. The result of this test will not be presented in this document since such data does not reflect the actual drive performance as a result of the load being shared by another drive. However, the second test was conducted with the drive operating in isolation and data were collected every 10 seconds for a 5-minute period. The results of this test will be presented and discussed in this chapter.

For both tests, data for voltages, currents, power profile and speed were collected from both the stator and the rotor. The tests were repeated for different operating speeds, (870, 820, 800, 780, 760, 740, 720, 700 r/min). An attempt to conduct the tests at lower speeds failed due to high oscillations in speed due to very low load torques.

3.2 Test Setup

Fig. 3.1 below, is a schematic of the equipment set-up used for this test. The two sets of data acquisitions employed consist of a power analyzer (DMMP), a personal computer (PC) and associated software. An additional dc voltmeter with serial communication port was employed in conjunction with the stator data acquisition system for recording speed voltage.

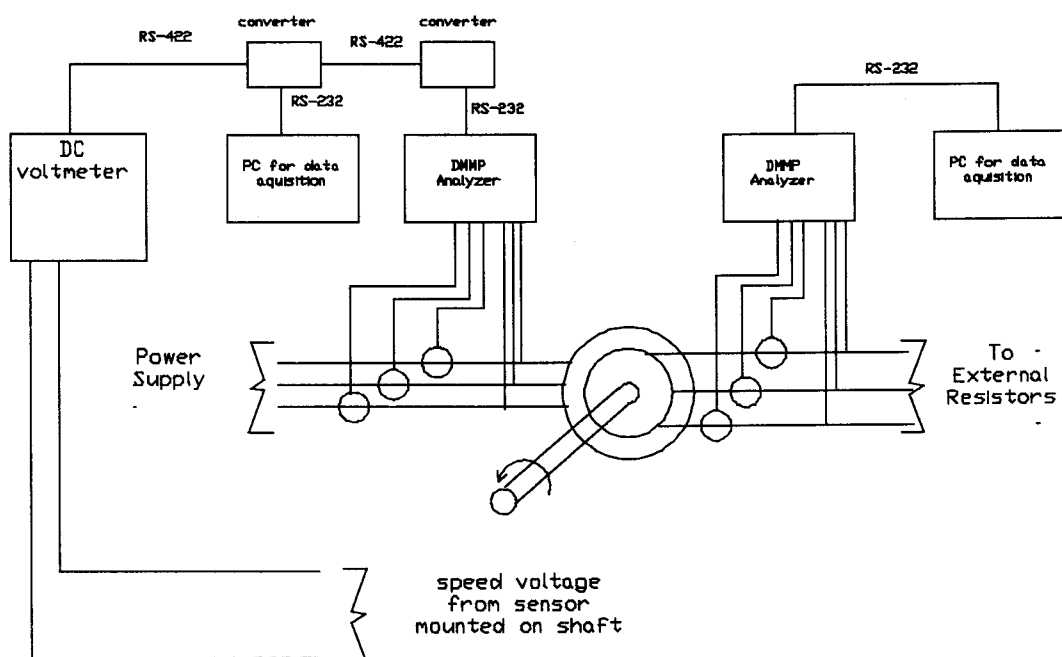


Figure 3.1 Existing drive test set-up

The stator and rotor line voltages, currents and speed are recorded and the associated phase voltage, watts, vars, va, power factor and frequency are derived and

recorded by the program at the instant of polling. Recording occurs at the predetermined interval (10-sec) for the duration of the test (5-min). The first test was conducted at the drive full load rated speed (870-rpm), wet well level at 192-ft above sea level and full speed flow of 7-MGPD. The test program was concluded at the lowest possible speed that could be achieved (680-rpm), wet well level at 193.5 and plant flow of 1-MGPD. The collected data were then converted into a spreadsheet and a complete analysis was made.

3.3 Analysis

The data collected above were averaged over the test duration as can be seen from the sample sheet in Appendix-III. These averages are then compiled in one sheet showing the average quantities (voltages, currents, power, frequency) and their corresponding speeds for both the stator and the rotor, Appendices-IV and V respectively. Due to the unbalance in the measured voltages and currents they were recalculated as

$$V_p = \sqrt{\frac{(V_a^2 * V_b^2 * V_c^2)}{3}} \quad (3.1)$$

and similarly for the currents

$$I_p = \sqrt{\frac{(I_a^2 * I_b^2 * I_c^2)}{3}} \quad (3.2)$$

where $V_a, V_b, V_c, I_a, I_b, I_c$, are the measured voltages and currents.

The stator and rotor resistances were separately measured across the winding terminals to be .16 and .19 ohms respectively. The corresponding phase resistances were calculated to be .08 and .095 ohms, based on the assumption of a Y-connected balanced winding assumption. The stator and rotor copper losses were calculated as

$$P_{cul} = 3 * I_p^2 * r \quad (3.3)$$

The rotor powers calculated by the data acquisition system reflect the power consumption by the external resistors based on the measurements. Figure 3.2 below shows the per-phase equivalent circuit and the associated measurements.

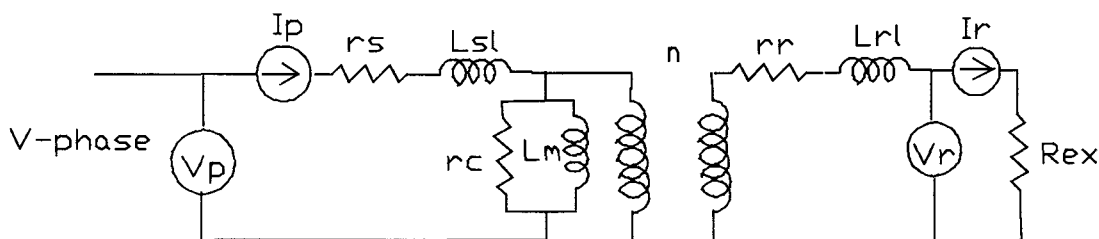


Figure 3.2 Per phase equivalent circuit and associated measurements

From rotor external power and from the rotor phase current, the external resistor corresponding to the particular test speed was calculated as

$$R_{ex} = \frac{P_{ex1}}{3 * I_r^2} \quad (3.4)$$

The output power can be calculated as per the following power flow diagram.

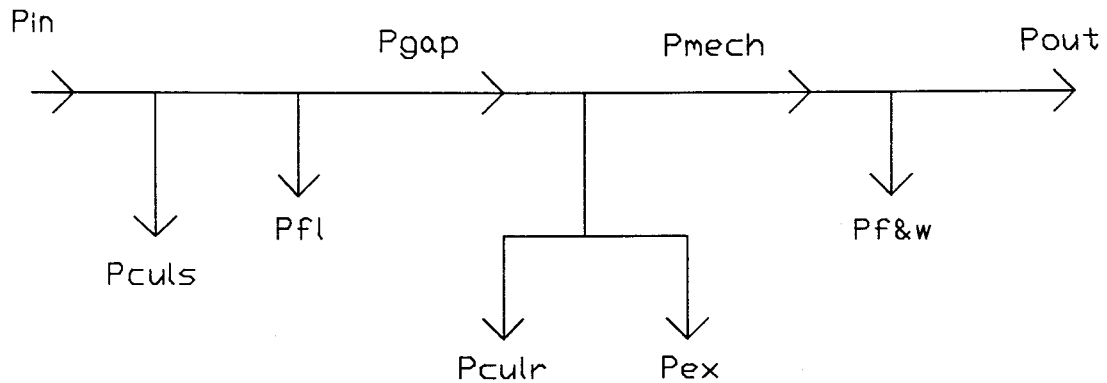


Figure 3.3 Drive power flow diagram

The machine iron losses cannot be measured directly but has been assumed to be a constant 2.5 percent of the motor rating, a typical value for this machine rating.

$$P_{fl} = .025 * P_{rated} \quad (3.5)$$

The friction and windage is dependent on speed and can be assumed to be 2.5 percent of the input power at that particular speed.

$$P_{fw} = .025 * P_{input} \quad (3.6)$$

The output power can be calculated as

$$P_{out} = P_{input} - P_{cuis} - P_{fl} - P_{culr} - P_{ex} - P_{fw} \quad (3.7)$$

and the machine efficiency, in percent, is found from input and output power as

$$\eta = \frac{P_{out}}{P_{input}} * 100\% \quad (3.8)$$

The motor developed torque at the various speeds is found from

$$T_e = \frac{P_{out}}{\omega} \quad (3.9)$$

where P_{out} is in watts and speed ω in rad/sec. The complete calculation results for all test speeds are attached in Appendix-VI. The resulting drive performance is shown below in Figs. 3.4 - 3.7.

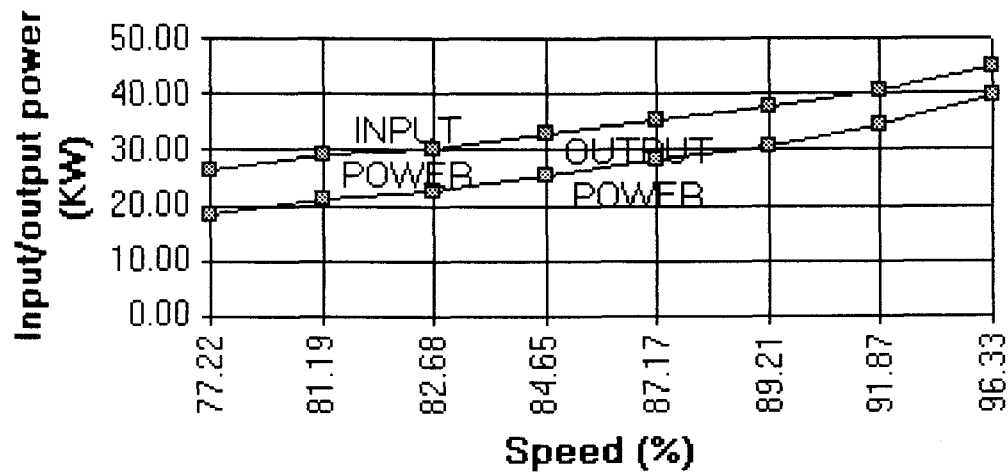


Figure 3.4 Existing drive input/output power

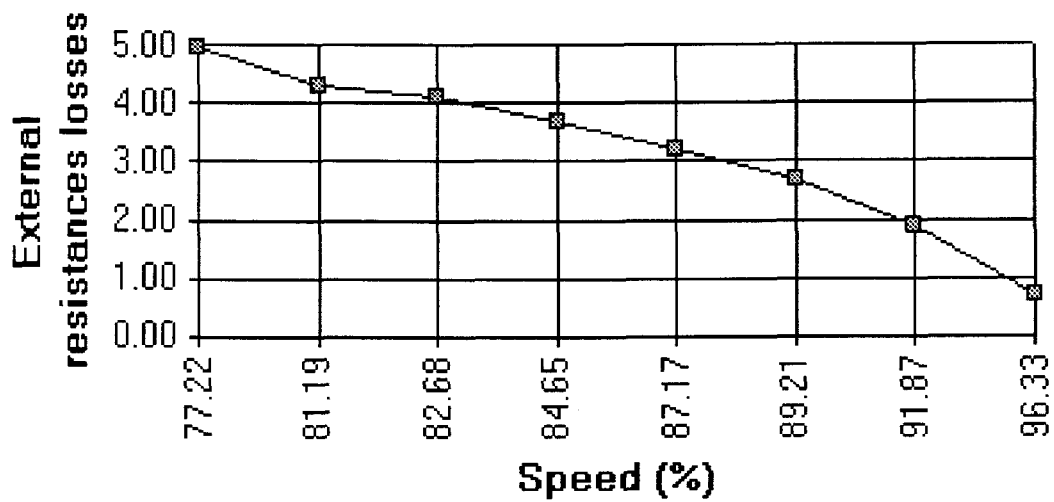


Figure 3.5 Existing drive external resistor losses

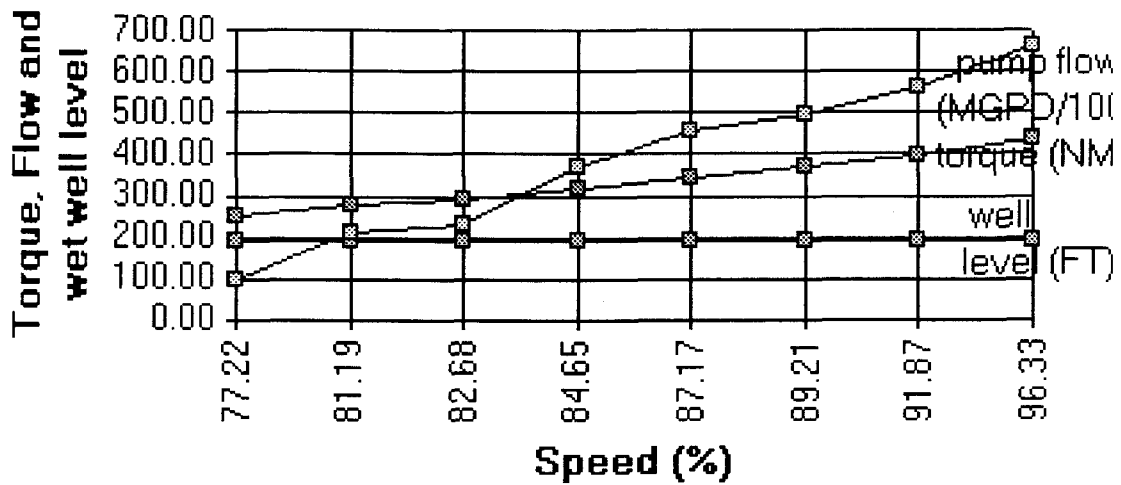


Figure 3.6 Existing drive and pump performance

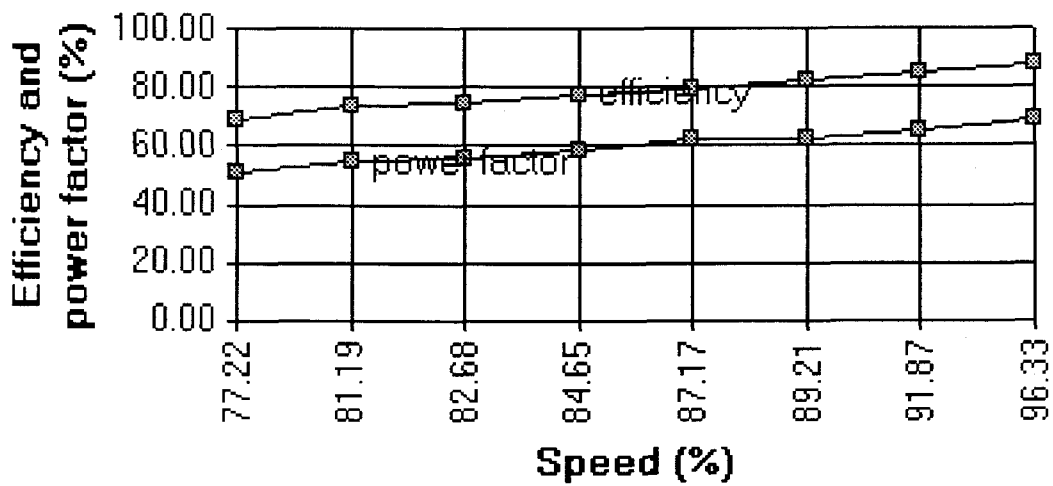


Figure 3.7 Existing drive performance

4. Design of Brushless Doubly Fed Machine

4.1 Background

The design process of any machine involves the determination of the dimensions and the electrical and magnetic particulars of that machine to satisfy given specifications which include horsepower, speed, efficiency, power factor, temperature and type of service[8]. In designing commercially available and established machines, such as induction motors, the design process is more practical since tabulated values are widely available and the designer's task is relatively simpler[9]. For special purpose machines though, including some of the highly specialized and commercially available machines, the task of the designer is somewhat more complex and a customized design process is required. The Brushless Doubly Fed Machine (BDFM) is a special type of a machine due to the existence of two windings on the stator side and the customized cage-like rotor[1,2,3]. This in turn requires a design process which can satisfy the special structure and operation requirement of this hybrid machine.

The BDFM stator consists of two windings which can be considered as two separate induction machine windings utilizing the same iron, sharing the same slot and contained in one frame. Therefore, the standard design process for the induction machine can be utilized here with some modifications and by adding more constraints. The constraints include slot dimensions requirements, instantaneous flux density considerations, operational speeds, horsepower ratings etc.. The BDFM rotor design on the other hand, is significantly different from that of an induction machine and a customized design process for the rotor is required.

The similarity in structure and operation between BDFMs and induction machines dictates the careful examination of the manufacturing process of the latter. Generally, the manufacturing of small and medium size induction machines uses standardized frames which cover a wide range of machine sizes and speeds. Therefore, a limited number of frames can accommodate different requirements of designs satisfying various ratings, speeds and voltages. Various machine sizes are accommodated in a particular frame by adjusting the core diameter and the lamination stack (axial length) [8]. Moreover, manufacturers rate a frame by its 4-pole, 1800 rpm, 60-Hz, maximum horsepower in order to standardize as much as possible of a design range[8, 9].

On the other hand, the ideal design of a machine involves the determination of all variables (bore diameter, axial length, number of stator/rotor slots, slot dimensions, number of turns, conductors sizes, flux densities, current densities and stator losses) for specific horsepower, voltage, frequency and speed and subject to a specific electric and magnetic loadings. The stator/rotor lamination are then fabricated to satisfy the above dimensions and a frame-size is then selected or fabricated to house these lamination. The design will be unique for this particular machine, and re-use of this design to accommodate different size machines will be limited.

In this chapter, the ideal design procedure is discussed in detail. Later, the main points of the practical design will be presented. The main difference between the two procedures, however, is that in the latter one, physical dimensions of frame and lamination details are known while they ought to be determined in the case of ideal design.

4.2 BDFM Design Procedure Overview

As mentioned above, the BDFM is a machine which consists of two induction machine windings, 6-pole power winding and 2-pole control winding, on the stator and a customized cage like rotor as can be seen from figure 4.1. The special rotor structure is required so as to obtain good coupling with each of the two stator windings [10].

In brief, the ideal design procedure for the BDFM begins by designing a 6-pole winding stator for an induction machine. This involves the determination of the bore diameter and axial length, slot specifics, conductors details and so on. At this point, a conservative air-gap flux density is assumed in order to obtain these details. The dimensions (D , L_a , d_s , w_s , w_t) corresponding to bore diameter, axial length, slot width and tooth width respectively, are then utilized to design a 2-pole winding stator of an induction machine. In the 2-pole winding design, the flux densities are calculated from

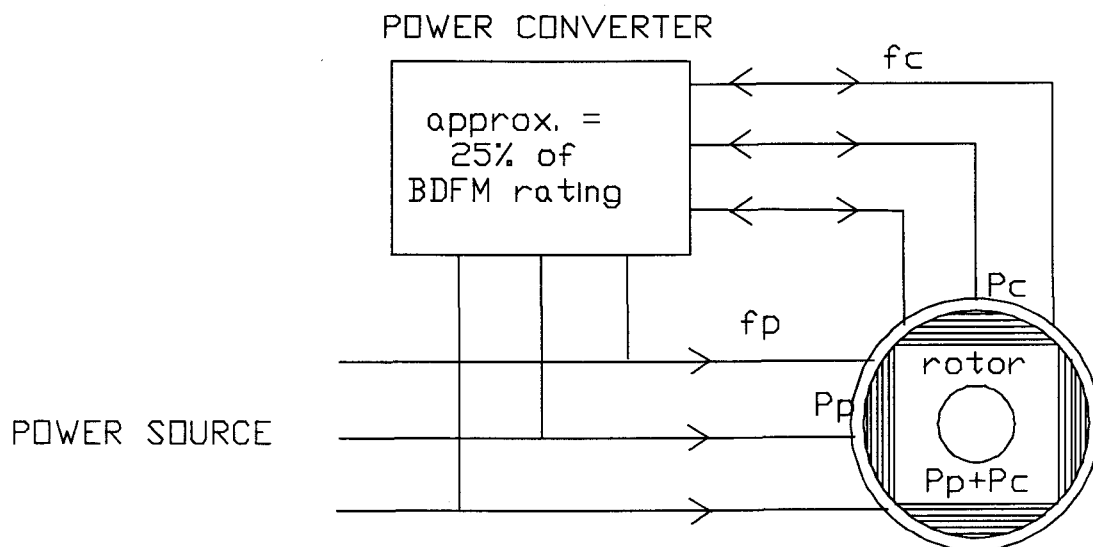


Figure 4.1 Brushless doubly fed machine (BDFM) drive

the available dimensions and other design parameters as will be shown later in this chapter. Since both windings utilize the same iron, the design process monitors any over saturation in both the teeth and the core due to the instantaneous sum of fluxes of both windings. In both cases suitable current densities were assumed in order to obtain conductor sizes.

Empirical data for induction machines were utilized in the above stator design process. However, during rotor design, the process begins by assuming a uniform rotor bars size and identifying the bar resistivities. These values along with others from the stator design, are used to predict the actual rotor loop currents utilizing the general BDFM machine variable simulation program [3]. Next, a relatively uniform current density is assumed for the rotor bars and hence the actual bar sizes are determined. The design is completed by determining the sizes of the different rotor slots and the and by calculating the machine efficiency.

4.3 Machine and Winding Ratings

Before beginning the design procedure, the drive and winding ratings shall be determined. This BDFM is designed to replace the existing (CWWT), 60-HP, 3-phase, 460-volts, 900-r/min pump drive located in Corvallis Waste Water Treatment Facility. Therefore, the rating of this machine will be the same as that of the pump drive and the required operational speed range is 600 to 900 rpm.

For an induction machine, the winding rating is the same as the of machine rating and is dictated by the application of the drive. In the BDFM, the machine rating will still be dictated by the particular application as mentioned above as in the induction machine. However, the winding ratings will be different.

To determine the winding ratings, the BDFM and induction machine speeds, frequencies and number of poles shall be investigated. For the BDFM the mechanical speed is obtained from,

$$N = 60 * \frac{f_p \pm f_c}{P_p + P_c} \quad (4.1)$$

or in r/sec

$$f_m = \frac{f_p \pm f_c}{P_p + P_c} \quad (4.2)$$

where

p_p = power winding number of pole pairs

p_c = control winding number of pole pairs

f_p = power winding supply frequency (Hz)

f_c = control winding supply frequency (Hz)

f_m = mechanical speed in r/sec

N = synchronous speed (r/min)

The rotor frequency is related to the power winding frequency, number of poles and the mechanical speed by

$$f_R = f_p - P_p * f_m \quad (4.3)$$

where

f_R = rotor frequency (Hz)

For the induction machine winding the mechanical speed is obtained from;

$$N=120 * \frac{f}{P} \quad (4.4)$$

where P =number of poles

The first three formulas came about due to the special structure of the BDFM rotor and its unique interaction with the stator windings and their derivation can be found in [1 - 5]. Therefore to satisfy the speed range required by the application, and from equation-4.1, with the power winding frequency being fixed to supply frequency 60-Hz, the control winding supply frequency must range between -20 and 0-Hz. When f_c is zero, the BDFM synchronous speed, 900-r/min, is achieved and when f_c is -20 the lower design speed limit, 600-r/min is achieved.

The control winding effect can be viewed as either aiding or working against the power winding. In the former one, power is being pumped into the control winding via the power converter and BDFM operates in super-synchronous speed, 900-r/min and above. In sub-synchronous speed, below 900-r/min, the control winding effectively operates to extract energy from the machine and pump it back into the line via the converter. For this application, the required operational range is in sub-synchronous speed and hence the control winding is generating power.

At the upper speed limit, application rated speed, the power winding is required to deliver the machine rating, 60-hp while the control winding is required to extract approximately 0-hp. At the lower speed limit, it is required that the control winding extract the most power. The control winding rating at the lowest speed limit can be computed from the converter rating formula as follow;

$$S_c \leq S_m * \frac{\hat{f}_c}{f_p + \hat{f}_c} \quad (4.5)$$

$$\hat{f}_c = 20 \text{ Hz}$$

where

S_c =converter rating

S_m =machine rating

Which means that for a 60-hp machine, the control winding shall be rated at 15-hp. Note that these ratings are required at speeds different than the synchronous speeds of the two equivalent induction machine windings. Therefore, the equivalent induction machine winding ratings shall be scaled up based on the difference in speeds. The horsepower hp of an induction machine winding is related to speed and other parameters by the following [11]:

$$hp = \frac{D^2 * L_a * B_g * Q * N * d * \eta * \cos \theta}{4.07 * 10^{11}} \quad (4.6)$$

or, in general, and by requiring that all other parameters other than speed remain constant

$$hp = K * N \quad (4.7)$$

where

D=bore diameter (inch)

L_a =axial length (inch)

B_g =air-gap flux density (lines per square inch)

Q=ampere-conductor per inch

d=winding distribution factor

η =efficiency

$\cos\theta$ =power factor

K=constant

Another approach, is to require that the BDFM winding develops the same torque at its synchronous speed as would its induction machine equivalent. That is; the torque due to the 6-pole winding remains the same at both BDFM and the equivalent induction machine synchronous speeds. Therefore from the torque, power and speed relationship

$$hp = T * n \quad (4.8)$$

where

T=torque (Nm)

n=speed (rad/sec)

or from Equation-4.7, the equivalent induction machine winding rating can be calculated from;

$$\frac{hp1}{N1} = \frac{hp2}{N2} \quad (4.9)$$

or

$$hp2 = \frac{hp1 * N2}{N1} \quad (4.10)$$

where for the power winding,

hp1=horse-power at BDFM natural speed (900 r/min)

N_1 =BDFM natural speed (r/min)

hp2=equivalent induction machine horse-power

N_2 =equivalent induction machine synchronous speed (1200 r/min)

while for the control winding,

hp1=horse-power at BDFM lower speed limit (600 r/min)

N_1 =BDFM lower speed limit (600 r/min)

hp2=equivalent induction machine horse-power

N_2 =equivalent induction machine synchronous speed(3600 r/min)

Therefore the power and control windings ratings based on the above formula, will be 80-hp and 90-hp respectively.

The supply voltage to the power winding is fixed to the line voltage, which is 460-volts, while the control winding voltage requires a constant volt per hertz ratio. Since the maximum control winding frequency is 20 Hz at 600 r/min, the control voltage at this condition will be 460 volts. The voltage of the equivalent 2-pole induction machine will be 1380-volts based on the volts per hertz rule. That is

$$\frac{V}{f} = \text{CONSTANT} \quad (4.11)$$

The following schedule shows the relationships between both windings frequencies, synchronous speeds, mechanical speed, supply voltage and the rotor frequency.

CONTROL FREQUENCY, f_c , Hz	-60	-40	-20	0	20	40	60
IM SPEED @ f_c , rpm	-3600	-2400	-1200	0	1200	2400	3600
POWER FREQUENCY, f_p , Hz	60	60	60	60	60	60	60
IM SPEED @ f_p , rpm	1200	1200	1200	1200	1200	1200	1200
f_m , rev/sec	0	5	10	15	20	25	30
MECHANICAL SPEED, rpm	0	300	600	900	1200	1500	1800
CONTROL VOLTAGE, volt	1380	920	460	0	460	920	1380

Figure 4.2 BDFM- frequency and speed schedule

The winding ratings are summarized in the following tables based on the above discussions.

Parameter	power winding	control winding
horsepower	60	15
voltage	460	460
speed (rpm)	900	600
frequency-Hz	60	-20

Table 4.1 BDFM windings rating

Parameter	power winding	control winding
horsepower	80	90
voltage	460	1380
speed (rpm)	1200	-3600
frequency-Hz	60	-60

Table 4.2 Equivalent induction machine winding ratings

4.4 Six Pole Winding Design

The ideal design process for the BDFM starts by designing the stator for the 6-pole, 1200-rpm, 3-phase, 60 Hz power winding at the equivalent horse power ratings (80-hp) shown in table-4.2. In addition to these known quantities given in that table, the design shall be carried out for an objective efficiency and power factor corresponding to this rating. These values can be obtained from established design data for general purpose induction motors found in various references. The graphs below are reproduced from similar ones given by Still and Siskind [11]. The first one provides the approximate power factor (%) versus the brake horsepower, and the efficiency (%) against brake horsepower is given below.

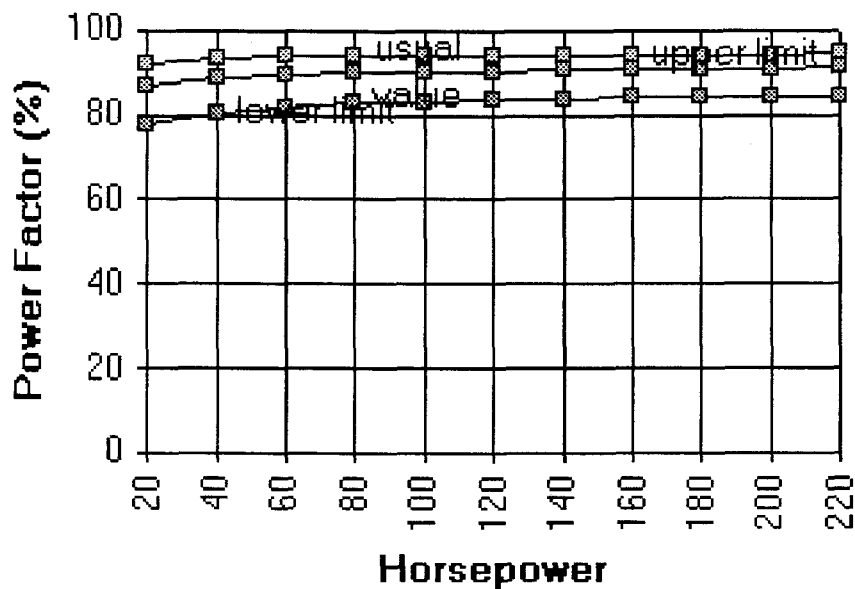


Figure 4.3 Power factor variation of 3-phase induction motor (at 100% rated load)

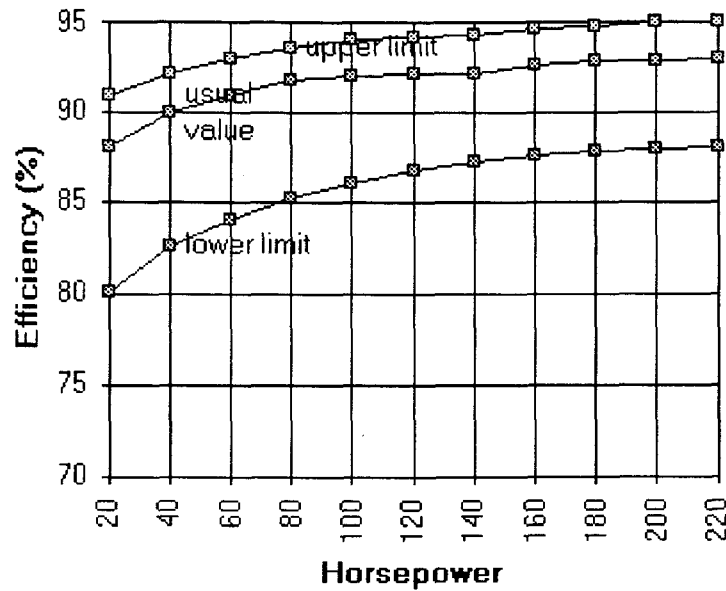


Figure 4.4 Efficiency variation of 3-phase induction motor (at 100% rated load)

4.4.1 Magnetic and Electric Loadings (B_g , Q)

The magnetic and electric loadings are the two design constraints which are monitored throughout the design process and their values dictate the machine particulars. The air-gap flux density B_g , constitutes the magnetic loading and shall be moderate to avoid excessive teeth and core saturation. The average value of the air-gap flux density over the pole pitch is defined as;

$$B_g = \frac{\Phi}{\tau * L_a} \quad (4.12)$$

where

Φ =the total flux lines per pole

τ =the pole pitch

The maximum tooth density is related to the air-gap flux density by;

$$B_{tm} = \sqrt{2} * B_g * \frac{\lambda}{wt} \quad (4.13)$$

where

λ =slot pitch

wt =tooth width

and the core flux density is related to air-gap flux density by

$$B_c = \frac{\frac{\Phi}{2}}{L_a * crd} \quad (4.14)$$

since only half of the flux produced by a pole flows in the core. So by substituting for Φ from equation-4.12

$$B_c = \frac{B_g * \tau}{2 * crd} \quad (4.15)$$

where

crd =core depth behind the slot

Therefore higher values of air-gap flux density B_g will lead to higher values in teeth and core densities which in turn produce higher iron losses, as will be shown later. Moreover, the magnetizing currents are also dependent on flux densities and it is usually desirable to keep the magnetizing component of the stator current as small as possible.

The usual values of B_g for 60 Hz excitation, lies between 23,000 and 38,000 lines per square inch with 26,000 as common value [11,12]. Higher values occur in

machines of larger output and diameter and lower voltage and number of poles. As a rule, the higher the flux in the teeth, the wider the teeth and the narrower the slots shall be made. Furthermore, different values of flux densities leads to various torque characteristics.

The additional constraint which shall be considered in BDFM design is the presence of the two windings which produce two fluxes in the same iron. It is the instantaneous sum of flux densities due to both windings which shall be monitored and kept within the above range limits compared to the flux due to one winding as in induction machine design. Therefore it will be wiser to design the 6-pole winding with a more conservative assumption of an air-gap flux density in the beginning in order to account for the 2-pole winding contributions later in the design. Note that a different air-gap flux density will be recalculated later in the design, the value of which will be considered as the design value. The variations between both quantities are due to assumptions and rounding functions made in the process of determining the machine physical dimensions and the number of conductors per slot. Refer to Appendix-X, the ideal design spreadsheet, items 11 and 46, for details.

The ampere-conductors per unit length (Q) of the periphery of the air-gap is referred to as the electrical loading and is directly proportional to the I^2r losses. Its value is dependent on machine size, voltage and type of ventilation. The value of Q is obtained from established tables and is related to the number of conductors, conductor currents and bore diameter by the following equation:

$$Q = \frac{C_s * I_p}{\lambda} \quad (4.16)$$

where

C_s =number of conductors per slot

I_p =phase current

The graph below was reproduced from a similar one given by Still and Siskind and it provides curves for the approximate values for stator ampere-conductors per inch of the air-gap periphery of induction motors.

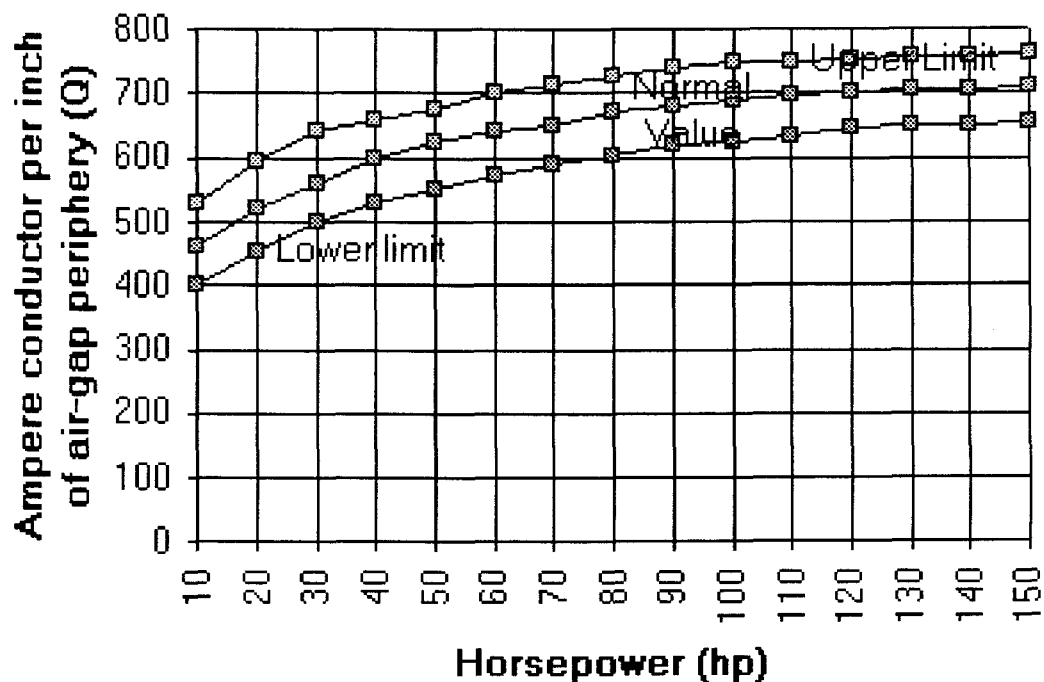


Figure 4.5 Electric loading of air-gap periphery of induction motor

4.4.2 Stator Slot Calculations

Generally the stator slot selection depends on the number of slots per pole per phase (nspp) and the rotor slots used (nr). In induction motor design, the slot per pole per phase shall be greater than or equal to 2 for either winding, to avoid excessive leakage reactance [8,12]. Furthermore and for satisfactory results in induction motor

operation, it has been proven that the number of stator slots shall not be equal to the number of rotor slots and that the difference between them shall not be:

equal to or a multiple of $\pm 3p$

equal to $\pm (p, 2p, 5p)$

equal to $\pm (1, 2, p+1, p+2)$

where

p = number of poles

The last three combinations were proven to cause motors to cog, develop synchronous cusps in the torque-speed curve or operate noisily respectively [8,11,12]. These effects are largely due to air-gap harmonics found in the flux wave due to the relative positions of the stator and rotor slots.

There are two types of BDFM proven rotor structures for a 6-pole/2-pole machine as will be shown later. The first one consists of 4-nests and each nest consists of a number of loops which are contained within a cage. The other type consists of only the four nests and their loops. Therefore, the BDFM rotor slots can only assume certain numbers. The table in Appendix-VII compares various stator-rotor slot number combinations against the above restrictions to determine the best combination for the design.

The stator slot number selected for this application is 72 which meet both criteria above and is common for equivalent induction motors of the same ratings. (refer to stator/rotor slot combination table in Appendix-VII).

4.4.3 Winding Factor (d)

For induction machines, double layer windings, Y connected, semi-closed slots, short chorded coil-span and lap type coils are the most common. In this BDFM design, a fractional pitch of 5/6 was implemented for both windings as can be seen from the winding layout schematics shown in Appendices-VIII and IX.

Since this is a distributed winding with at least 4-slots per pole per phase which employs a fractional pitch of 150/180, the winding factor is calculated as the product of the winding distribution factor and the pitch factor.

$$d = f_d * f_p \quad (4.17)$$

where

f_d =winding distribution factor

f_p =winding pitch factor

The distribution factor can be calculated from the slot pitch in (electrical degrees) and the number of slots per pole per phase (nspp) as follow;

$$f_d = \frac{\sin(nspp * \frac{\beta}{2})}{nspp * \sin(\frac{\beta}{2})} \quad (4.18)$$

where

β =slot pitch in rad

The pitch factor can be computed based on the coil span and the number of layers of the winding as follow;

$$f_p = \sin\left(\frac{\gamma}{2}\right) \quad (4.19)$$

where

γ =coil span in electrical degrees
2=for double layer winding

So for the 6-pole winding the slot pitch in electrical degrees is 15, the coil span is 150 and the number of slots per pole per phase is 4. This gives a distribution factor of .958, a pitch factor of .966 and the winding factor of .93 as can be seen from the design sheet.

4.4.4 The Physical Volume of The Machine ($D^2 * L_a$)

The output equation of a polyphase motor is

$$HP * 746 = 3 * E * I_p * \cos\theta * \eta \quad (4.20)$$

where

E=phase voltage
 I_p =phase current

The derivation of the phase voltage involves calculating the induced voltage in a number of turns due to the flux per pole. The flux cut per revolution is

$$= \Phi * P * N \quad (4.21)$$

and per second

$$= \frac{\Phi * P * N}{60} \quad (4.22)$$

The average value of induced emf in the number of series conductors per phase for a distributed chording winding is

$$E_{av} = \frac{d * Z * \Phi * P * N}{60 * 10^8} \quad (4.23)$$

where

Z=number of conductors per phase

Φ =total flux per pole in lines

on the assumption of a sine wave flux distribution, the form factor is 1.11 and the rms value of the induced voltage after substituting for (P*N) by (120 *f) is

$$E = 2.22 f * d * \Phi * Z * 10^{-11} \quad (4.24)$$

The same equation can also be derived from the total flux per pole, under the assumption of a sinusoidal flux waveform, as follow;

$$\phi(t) = \Phi * \sin(\omega * t) \quad (4.25)$$

where

Φ =peak flux

$$\omega = 2\pi f$$

The induced voltage due to this flux is

$$\begin{aligned} e(t) &= N_s * \frac{d\Phi}{dt} \\ &= 2 * \pi * f * N_s * \Phi * \cos(\omega * t) \\ &= E_m * \cos(\omega * t) \end{aligned} \quad (4.26)$$

where

N_s = number of turns per phase

E_m = peak emf

$$E_m = 2 * \pi * f * N_s * \Phi \quad (4.27)$$

The rms of which

$$\begin{aligned} E &= \frac{E_m}{\sqrt{2}} \\ &= \frac{2 * \pi}{\sqrt{2}} * f * N_s * \Phi \\ &= 4.44 * f * N_s * \Phi \end{aligned} \quad (4.28)$$

since there are 2-conductors per turn, and by including the winding factor for distributed winding, E becomes

$$E = 2.22 * f * d * Z * \Phi \quad (4.29)$$

The flux can be represented in terms of the machine dimensions and flux density as follows;

$$\Phi = B_g * \frac{\pi * D * L_a}{P} \quad (4.30)$$

from equation-4.4 above, the frequency is

$$f = \frac{P * N}{120} \quad (4.31)$$

by substituting for flux and frequency in equation-4.29, the phase voltage can be expressed as

$$E = 5.81 * N * B_g * D * L_a * d * Z * 10^{-10} \quad (4.32)$$

The electrical loading ampere-conductors per inch of the air-gap periphery is defined as

$$Q = \frac{3 * Z * I_p}{\pi * D} \quad (4.33)$$

solving for I_p

$$I_p = \frac{Q * \pi * D}{3 * Z} \quad (4.34)$$

and by substituting for E from equation 4.32, and I_p from 4.34 in the output equation-4.20 and solving for the physical volume ($D^2 L_a$) we get

$$D^2 * L_a = \frac{4.07 * HP * 10^{11}}{B_g * Q * N * d * \eta * \cos\theta} \quad (4.35)$$

This value has to be split into its components, the machine physical dimensions.

4.4.5 Diameter and Axial Length Determination (D , L_a)

The method of determining the physical dimensions of stator bore and lamination stack length is generally not unique in contemporary machine design. However, one of the simplest ways of determining these dimensions, is to consider what is called the square polar law [8,11,12]. That is, the closer the pole face to a square (pole pitch=axial length), the better the design becomes. Further, the general practice is to restrict the diameter more than the axial length due to the limited standard frame sizes available.

In the BDFM case, the two windings present in the same frame provides a bigger challenge in choosing these dimensions. However, based on their pole numbers, there will be more flux associated with the 6-pole winding compared to that of the 2-pole winding. Also, smaller diameters are anticipated for the 2-pole winding compared to that of the 6-pole which in turn may lead to thinner teeth, due to the requirements to accommodate the conductors of both windings. This may compromise the mechanical strength of the teeth. Therefore, it will be wise to employ the square polar law in designing the 6-pole winding since larger diameters and flux requirement are expected. Hence, for a square pole

$$L_a = \tau = \pi * D / P \quad (4.36)$$

where

τ =pole pitch

From equation-4.35 it was found that

$$D^2 * L_a = \text{constant} \quad (4.37)$$

Substituting for L_a in equation-4.37 from equation-4.36 gives

$$\frac{D^3 * \pi}{P} = \text{constant} \quad (4.38)$$

This gives the value of D , then by substitution in equations- 4.37 and 4.36, L_a and τ are obtained respectively. These values can be adjusted as necessary to adapt to any design limitations such as teeth width, flux density or frame size.

4.4.6 Number of Conductors Calculations (C_s , Z)

The number of conductors per slot can be derived from equation-4.34, by solving for the number of conductors per phase as follow;

$$Z = \frac{Q * \pi * D}{I_p} \quad (4.39)$$

for the 72-slot stator, there are 24-slots per phase and the number of conductors per slot C_s is obtained as;

$$C_s = \frac{Z \text{ (cond/phase)}}{24 \text{ (slots/phase)}} \quad (4.40)$$

substituting for Z from equation-4.39

$$\begin{aligned}
C_s &= \frac{Q}{I_p} * \frac{\pi * D}{24} \\
&= \frac{Q}{I_p} * \frac{\pi * D}{6} * \frac{1}{4} \\
&= \frac{Q}{I_p} * \frac{\tau}{4} \\
&= \frac{Q * \lambda}{I_p}
\end{aligned}
\tag{4.41}$$

I_p is the phase current and can be found from the output equation and λ is the slot pitch and is determined from;

$$\lambda = \tau / nspp \tag{4.42}$$

where

$nspp$ = number of slots per pole per phase.

The number of conductors per slot found from above must be an even number since a double layer winding is employed. Therefore, C_s must be rounded to the nearest even number during the design.

4.4.7 Slot and Tooth Width Determination

The slot and tooth widths are selected to accommodate the number of conductors (or substitute conductors) per slot and the tooth flux density, allowed without over-saturation of the iron, for both windings. The maximum apparent flux

density in the teeth ranges between (75K and 105K) lines per square inch [11]. Note that an assumption of a flux density here must take into account the flux density required for the 2-pole winding. This suggests that the slot and tooth widths determined in this part of the design can be modified later to account for the effect of the 2-pole design. From equation-4.24, the flux per pole is calculated as

$$\Phi = \frac{E \cdot 10^8}{2.22 \cdot d \cdot f \cdot Z} \quad (4.43)$$

The actual air-gap flux density corresponding to this flux can now be determined, to reflect any assumptions or rounding during the determination of the physical dimensions and the number of conductors, as follow;

$$B_g = \frac{\Phi}{\tau \cdot L_a} \quad (4.44)$$

Before determining the tooth width, a flux density in the teeth shall be assumed. The typical value is 85,000 lines per square inch [Still & Siskind]. The air-gap flux density can be related to teeth flux density by

$$\begin{aligned} B_{tm} \cdot A_t &= B_{gm} \cdot A_g \\ B_{tm} \cdot nspp \cdot wt \cdot L_a &= B_{gm} \cdot \tau \cdot L_a \\ B_{tm} \cdot wt &= B_{gm} \cdot \frac{\tau}{nspp} \\ B_{tm} \cdot wt &= B_{gm} \cdot \lambda \end{aligned} \quad (4.45)$$

where

$$B_{gm} = \sqrt{2} * B_g \quad (4.46)$$

and w_t is the tooth width, can now be calculated as

$$w_t = \frac{B_{gm} * \lambda}{B_{tm}} \quad (4.47)$$

It is important to note that the tooth flux density assumed here represents the apparent flux density and assumes that all air-gap flux passes through the teeth. Therefore the tooth width calculated here might be an oversize for a regular 6-pole winding induction machine. However, for BDFM design it will be advisable to oversize the tooth width calculated in the 6-pole design in order to anticipate the flux density due to the 2- pole winding. Other elements which might affect the selection of the tooth width include limitation on slot depth. Too wide of a tooth leads to narrow and deep slots which in turn will lead to a larger frame and hence to an expensive design. In all cases, the tooth flux density shall be recalculated to reflect any modification of tooth width. The slot width can now be calculated as

$$w_s = \lambda - w_t \quad (4.48)$$

Note that in this design a parallel sided tooth and semi-closed slot is assumed. Therefore the slot width determined above represent the width at the narrow end of the slot.

4.4.8 Conductors Sizes and Numbers

The number of conductors per slot were already determined above to satisfy a given electric loading. The sizes of these conductors can be determined by assuming a certain value of current density (Δ), which meets recent industrial standards for electrical winding insulations. This is generally between 3500 and 5000 amps per square inch. The conductor area (c_a) is then calculated from

$$c_a = I_p / \Delta \quad (4.49)$$

For smaller motors where shorter end windings are required, the wire area which was calculated above, can be substituted by a multiple, smaller number of conductors in parallel. The number of substitute conductors (C_{ss}) is determined from

$$\begin{aligned} C_{ss} * c_{as} &= C_s * c_a \\ C_{ss} &= \frac{C_s * c_a}{c_{as}} \end{aligned} \quad (4.50)$$

where

c_{as} = area of substitute conductors

Again the number of substitute conductors must be an even number since a double layer winding is employed. Furthermore, in this design, an integral number of uniform area substitute conductors is employed. Therefore the number of parallel conductors (p_c)

$$P_c = \frac{C_{ss}}{C_s} \quad (4.51)$$

must be an integer. This will lead to a different value of current density and care shall be taken not to exceed the upper limit suggested above.

4.4.9 Required Slot Depth

At this point, the required 6-pole winding slot depth can be calculated based on the number of substitute conductors and the slot width available for conductors. The procedure involves the determination of the slot width available for wires by subtracting the slot insulation thickness from the previously calculated slot width. The number of conductors which can be accommodated in parallel in the slot, width wise, and the number of rows of these parallel wires are then calculated. The slot depth is then calculated by adding up the depth of the wires stacked in the slot, together with the double layer spacer, slot lining and the allowance for spaces between wires. Refer to the schematic below and to Appendix-X for illustration and calculation formulas.

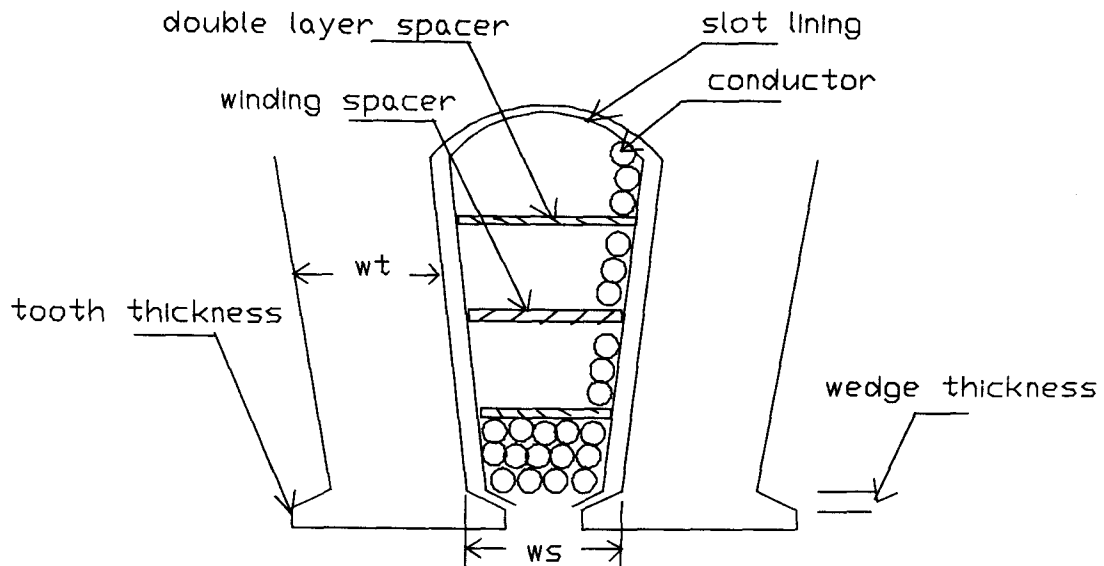


Figure 4.6 Slot and tooth layout

4.4.10 Number of Turns and Winding Resistance

For a 72-slots double layer winding, there are two coil sides per slot, 24-coils per phase and 4-coils per pole per phase. The number of turns per coil is determined from the number of conductors per slot found above. The number of turns per phase (N_s)

$$N_s = N_c * cph \quad (4.52)$$

where

N_c =number of turns per phase

cph =number of coils per phase

4.4.11 Winding Resistance and Copper Loss

One winding turn will travel twice the axial length and twice the end winding. The end winding length depends on the type of conductors used and the number of poles of the winding. Larger wire (lower AWG) is stiffer and hence requires a longer end winding. In addition, smaller number of poles require longer end windings due to a longer pole pitch. The mean length per turn can be calculated based on the following schematic derived from a similar one by Kuhlman [12] for diamond type windings.

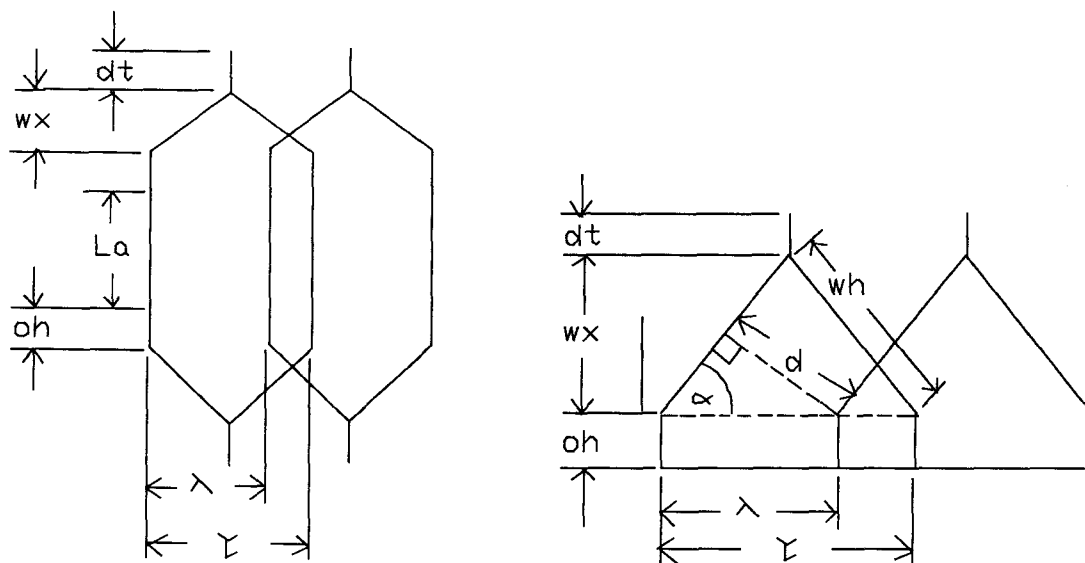


Figure 4.7 Winding length schematics

The angle α can be calculated as

$$\alpha = \sin^{-1}\left(\frac{dt}{\lambda}\right) \quad (4.53)$$

where

$$d_1 = w_{sm} + s \quad (4.54)$$

w_{sm} = slot pitch at the mean depth

s = 0.12 inch for 300-600 volts applications

Note that (d_1) represent the thickness of the coil plus the clearance between two adjacent coils at the end windings. The thickness of the coil may be assumed to be the same as the slot width at its mean depth, while the clearance is obtained from empirical data and its value varies with the applied voltage [12]. The slot pitch and width and the pole pitch at slot mean depth can be assumed to be equal to the slot pitch, width and pole pitch at the air-gap in the ideal design, since these dimensions are not known beforehand and the slot width is assumed to be uniform. However, in the practical design, the actual slot pitch at the mean can be calculated and a better approximation of the winding length is obtained.

The pole pitch at the mean of slot depth

$$\tau_m = \frac{\pi * (D + d_s)}{P} * c_p \quad (4.55)$$

where

P = number of poles

c_p = 5/6; per unit pitch of the coil

The horizontal part of one end of the winding (hw)

$$2hw = \frac{\tau_m}{\cos \alpha} \quad (4.56)$$

The over hang (oh) can be approximated to be equal to slot depth

$$oh = ds \quad (4.57)$$

and by discarding the diamond tip, since it will not be used in this application, the approximate mean length per turn can be calculated as follow:

$$mlt = 2 * L_a + 4 * ds + 4 * hw \quad (4.58)$$

and the total winding length per phase in feet is

$$wl = N_s * \frac{mlt}{12} \quad (4.59)$$

The specific resistance, r'_s , for a certain conductor in (ohms/1000 ft) @ 75 deg C can be obtained from established data books, [13], and the per phase resistance is calculated as

$$r_s = \frac{wl * r'_s}{1000 * p_c} \quad (4.60)$$

where

p_c = number of parallel conductors

The winding copper loss is found as

$$W_{cul6} = 3 * I_p^2 * r_s \quad (4.61)$$

where

$$I_P = \frac{746 * HP}{3 * E * \eta * \cos\theta} \quad (4.62)$$

Note that at BDFM's full load speed (900 r/min), the losses calculated above will be less since lower currents will be drawn at that speed.

4.4.12 Core Flux Density and Depth

Only half the flux per pole will flow in the core of the machine as can be seen from the graph below. The flux density corresponding to that flux must be within acceptable range (50,000 to 85,000 lines per square inch) to avoid excessive core saturation. This requires the proper sizing of the core depth (crd) behind the slot.

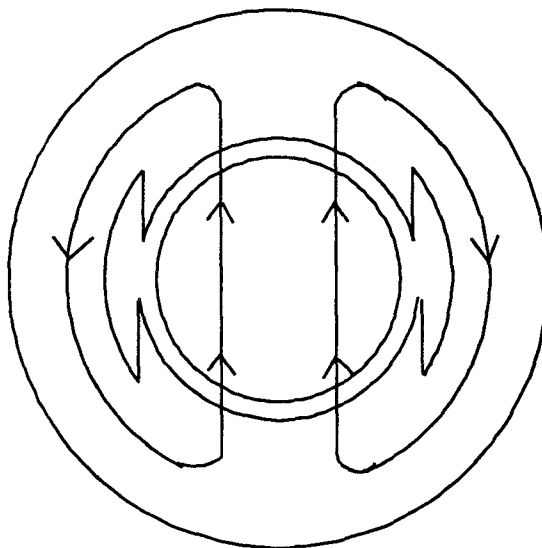


Figure 4.8 Polyphase machine flux path

Hence, by assuming a reasonable flux density at this point and by keeping in mind that only half the flux per pole flows through the core, a first estimate of core depth can be predicted to be

$$B_c = \frac{\frac{\Phi}{2}}{L_a * c r d} \quad (4.63)$$

The core depth can be calculated from above and the outside diameter can be determined. However, this will not be the design value since the 2-pole flux contribution was not considered at this point. Since the design was carried out on a spreadsheet a trial and error process can be implemented where various core depths are assumed and the core flux density flag, in the windings common calculations section, is monitored for over-saturation. In addition, the core depth determination will be influenced by the selection of a suitable frame size which puts a limit on the maximum outside diameter allowed.

4.4.13 6-Pole Winding Iron Loss

The iron loss includes losses due to teeth and core flux densities which are obtained by first estimating their corresponding weights. For USS, M-36 26 gauge, the density is .28 lb per cubic inch and the teeth and core weights are then calculated as

$$m_c = .28 * \pi * (D_o - c r d) c r d * L_a \quad (4.64)$$

for the core, and

$$m_t = .28 * wt * ns * ds * L_a \quad (4.65)$$

for the teeth.

The watts per pound factors are then obtained from established test data, similar to figure 4.9 below which was reproduced from USS Electrical curves for USS M-36 steel sheets, for the calculated flux densities above. The corresponding losses can be determined as shown in appendices-X and XI.

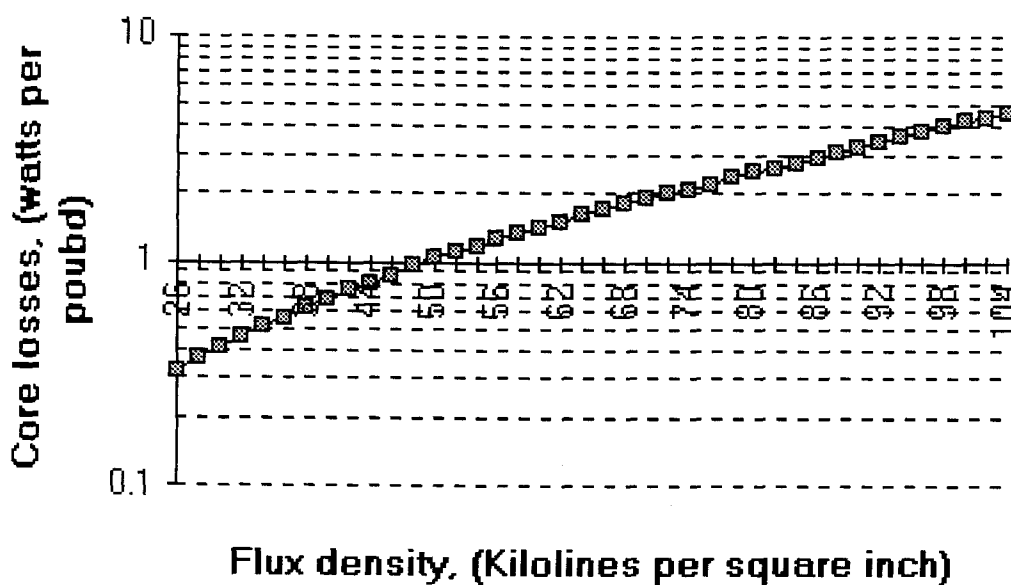


Figure 4.9 Iron losses per pound

This concludes the 6-pole winding design and the design the 2-pole winding follows. It is important to note that some of the values determined above may need to be recalculated in order to account for the 2-pole winding design.

4.5 Two-Pole Winding Design

The 2-pole winding design procedure is practically the same as that of the 6-pole winding. The difference is that the machine physical dimensions and slot and tooth width are known to us. Therefore, the flux density will now be calculated rather than assumed. However, the electrical loading (Q) will still be assumed from fig 4.5 above. The power factor and the efficiency for this design horsepower rating are also obtained from fig-4.3 and 4.4 respectively. Note that this machine will be designed to cause rotation in the opposite direction to that of the 6-pole winding. This will make the corresponding frequency and speed to be negative which will lead to negative fluxes and fields which rotate in the opposite direction.

Since BDFM natural speed direction is the direction of speed corresponding to the 6-pole winding, The 2-pole winding will be in the generation mode for the speed range specified for this design. The current calculated from formula-4.62, will be different in this case since mechanical power is the input and is converted to electrical power. The current in this case is given by

$$I_p = \frac{HP * 746 * \eta}{3 * E * \cos\theta} \quad (4.66)$$

With the air-gap flux density calculated from above, and the knowledge of the slot and tooth width from the previous section, the tooth flux density can be calculated as follow,

$$B_{tm} = \sqrt{2} * B_g * \frac{sa}{t} \quad (4.67)$$

where

sag= periphery surface area at air-gap

t_{sa}= teeth surface area

The same current density assumed for the 6-pole winding may be assumed here for determining the winding conductor sizes, then the corresponding slot depth required to contain them shall be calculated in the same way as previously shown in the 6-pole design.

4.6 Common Calculation For Both Windings

The common calculation for both windings includes the calculation of the stator total slot depth, monitors teeth and core flux densities and provides required information for the simulation program to be used in rotor design. In addition, a summary sheet which summarizes the design results is also included in this section.

The total slot depth required to contain both windings copper is calculated as

$$d_s = d_{s6} + d_{s2} + wdt + tt + s_{62} \quad (4.68)$$

where

d_{s6} =6-pole winding slot depth

d_{s2} =2-pole winding slot depth

wdt=wedge thickness

tt =tooth thickness

s_{62} =spacer between the two windings

Refer to fig-4.6 for illustration. Note that this depth assumes a uniform slot width

calculated in Section 4.5 at the air-gap periphery. The actual slot depth will be somewhat smaller when the slot shape shown in fig-4.6 is considered.

As indicated earlier, the flux densities in both teeth and core must be monitored to avoid any excessive iron saturation. This can be done by maintaining the instantaneous flux densities to be within the limits mentioned earlier. The 2-pole winding produces a negative flux waveform; that is a flux traveling in the opposite direction of the 6-pole winding flux waveform and at a different speed. The maximum instantaneous flux density corresponds to the instant in which both waveforms coincide in an aiding fashion as can be seen from the demonstration graph below.

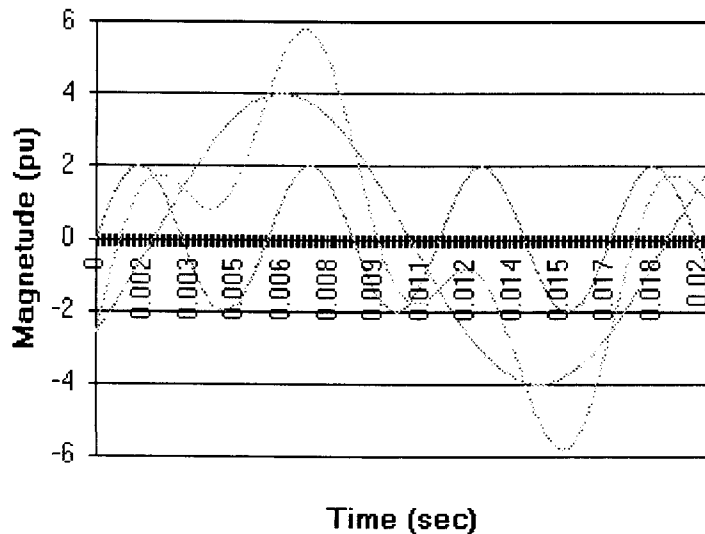


Figure 4.10 BDFM flux waves interactions

Therefore, the maximum teeth flux density is

$$B_{tm} = B_{tm6} + |B_{tm2}| \quad (4.69)$$

and the maximum core density is

$$B_{cm} = B_{cm6} + |B_{cm2}| \quad (4.70)$$

The absolute value is required to account for the negative sign associated with the 2-pole winding fluxes. Based on these peaks, the slot and tooth width, core depth and number of turns may need to be tuned in order to avoid excessive saturation. During the design of each winding, it was required to approximate a core depth to accommodate each winding flux profile. Either core depth may not accommodate the maximum instantaneous core flux density. Therefore, a suitable core depth must be chosen to satisfy the allowable limits and the frame size. Too large a core depth will lead to a larger frame size and increased cost. These modifications are easily accomplished since the design process was implemented on a spread sheet. Refer to Appendix-X and XI for illustration.

After the core depth is calculated, the outside diameter is calculated and then the suitable frame size is selected. For this ideal design and for an outside diameter of $D_o=22$ (in), the frame which has the closest dimensions to this is NEMA frame-445. The selection shall be made so as to minimize the change of the core depth calculated above.

4.7 BDFM Rotor Design

In order to support the two air-gap rotating fields of different pole number, due to the simultaneous excitation of the two stator windings, a special rotor structure is required [1 ; 5]. Two proven structures are capable of accommodating the two winding requirements; refer to graphs below. A cage like rotor which consist of four nests of isolated loops at one end of the rotor and connected to a common bar at the other end,

with the outer loops (cages) connected to the common rings at both ends. The other type consist only of the four nests of loops connected at one end, and is referred to as the cage-less type. Both types were previously built and tested as laboratory prototypes. The cage-less structure will be the subject of discussion in this design procedure.

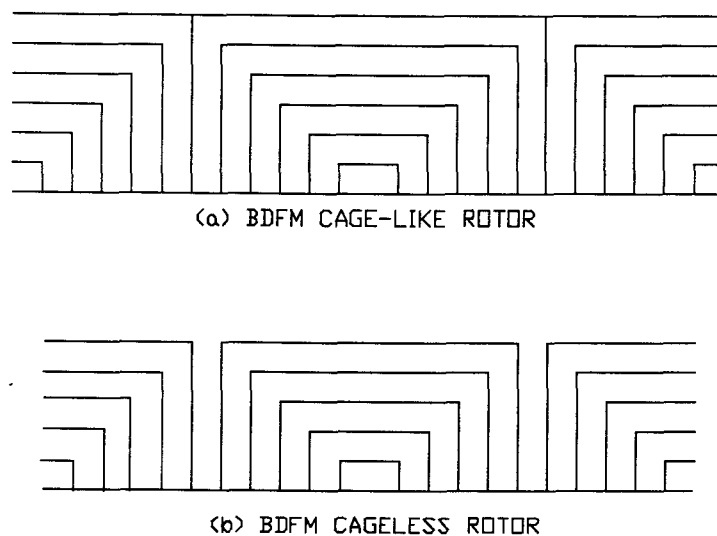


Figure 4.11 BDFM rotor structures

4.7.1 Preliminary Calculations

The number of nests mentioned above is determined by the combination of the pole pairs of the stator winding as was analytically showed by Creedy during the early development of the rotor structure for this kind of machine [14].

$$nst = P_p + P_c \quad (4.71)$$

This number can also be considered as the number of poles of the rotor. The selection of the number of rotor slots depends on the number of stator slots, the type

of rotor structure and the number of loops per nest used. In addition to the restrictions discussed in section 4.5.2, it was found that satisfactory results for induction machines, were obtained when the difference between stator and rotor slots is between 15 and 30 percent. Therefore, the rotor slot number is recommended to be between 50 and 94 , excluding $n_r=72$, which is the number of stator slots. The rotor structure selected can only assume some of the numbers within this range. For example, by selecting the cageless rotor, rotor slot numbers can be (56,64,80,88). The restrictions discussed in section 4.5.2 are then applied to select the suitable rotor slot number (n_r). In the following discussion and for illustration, $n_r=40$ is assumed.

The rotor diameter can be assumed to be equal to that of the stator bore, since the air-gap length is very small. However, and for completeness, the air-gap length was computed and the actual rotor diameter was used in the rotor design.

Most design books suggest that the air-gap length shall be as small as mechanically possible [8,11,12]. In addition, too large an air-gap ought to be avoided since it leads to the substantial increase in the magnetizing current. Khulman, suggests that the approximate minimum air-gap length can be determined from the empirical formula

$$l_g = .125 - \frac{10.17}{D+90} \quad (4.72)$$

therefore, the rotor diameter is

$$D_r = D - 2 * l_g \quad (4.73)$$

4.7.2 Rotor Bar Currents and Sizes

Due to the existence of the two stator windings and the unique rotor structure the values of the rotor bars currents are not uniform like those of induction motors. From previous simulation results and from experience with laboratory prototypes, it was evident that rotor outer loops carry higher current values compared to inner ones. In fact the current values increase gradually from the inner loops to the outer ones. With this fact in mind and by assuming a required uniform current density in all the loops, the rotor bars sizes that can satisfy that density can be obtained. This is no easy task if one begins from scratch, due to the difficulty in determining the rotor currents.

In the early development of the BDFM, a simulation program was developed to simulate the 36/44 stator/rotor slots combination, based on the knowledge of machine ratings, voltages, speed, coils specifics and so on. Later, this program was modified to accommodate any stator/rotor slot combination and any winding configuration. Therefore, the rotor currents were calculated from these simulation programs for an assumed uniform rotor bar area and based on the stator details discussed above. Note that the design sheet produces a summary sheet for use in the simulation program to obtain the rotor currents.

Customarily, the current density in rotor bars for induction motors ranges between 15% to 30% higher than that of the stator current density [12]. This is because no insulation is required for the bars and better ventilation exists; and hence higher temperatures are allowed. Based on this current density and the rms values of the individual loops currents, the corresponding bar cross sectional areas and dimensions are then calculated.

"x"= a sub-script used for loop designation throughout the rotor design,

$$ca_x = \frac{I_x}{\Delta_r} \quad (4.74)$$

(u,v,w,x,y,z,...)

The end-ring size is calculated based on the maximum current flowing in any section of the ring. This happens to be the innermost section corresponding to the innermost loop. The sum of all loop currents per nest, since they are all in phase, flow in that section thereby dictating the design to be carried out at that current level. Assuming the same current density as in the bars leads to the determination of the minimum end ring size and dimensions. Refer to the following figure and Appendices-X and XI for illustration and calculation details.

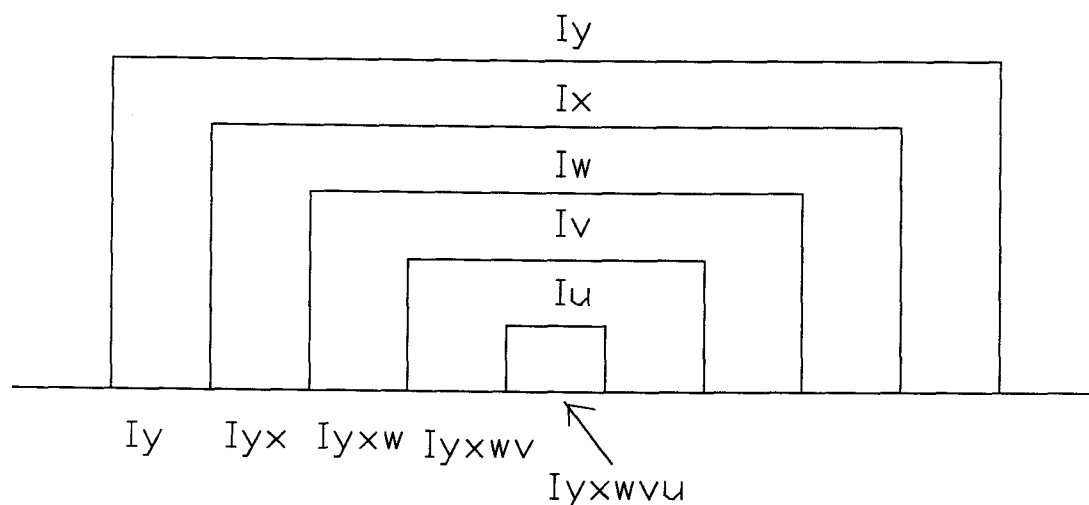


Figure 4.12 Rotor nest currents distribution

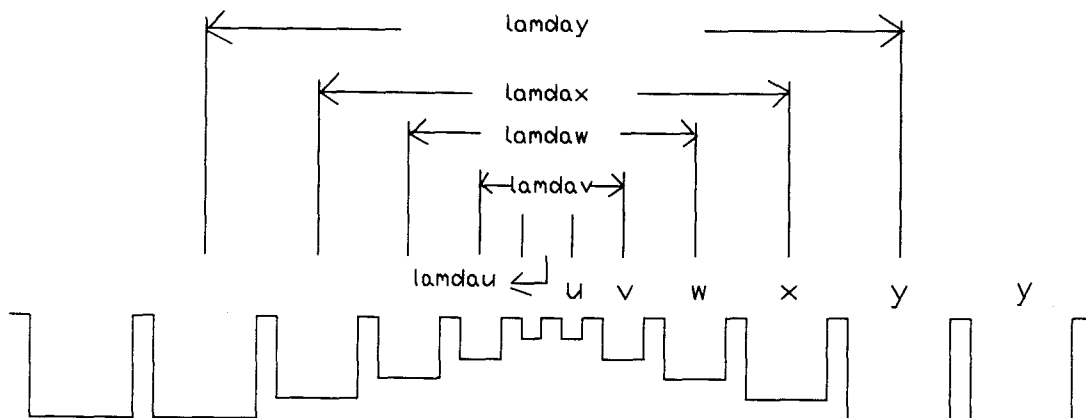


Figure 4.13 Rotor slot and tooth configuration

4.7.3 Slot and Teeth Width

Due to the non-uniformity in the conductors sizes of the rotor bars, the slot widths will also be non-uniform, unlike the induction machine. On the assumption of square bars to be used in this design, the slot widths can assume the corresponding bar width plus a tolerance.

$$w_{srx} = dia_x + .03 \quad (4.75)$$

where

x =bar designation, (u,v,w,x,y,...)

dia=bar width or diameter

Therefore the slot width is dependent on the bar size. The tooth width, however; can be assumed to have a uniform width and can be calculated from

$$w_{tx} = \frac{(\pi * D_r - 2 * nst * (w_{srx}))}{n_r} \quad (4.76)$$

and the corresponding slots pitches are calculated individually as shown in the design spreadsheet and as per fig 4.13 below. The following schematics shows the rotor lamination shapes which reflect the above discussions.

Similarly the slots depths will also be dependent on the bar sizes as

$$ds_x = dia + tt \quad (4.77)$$

where

tt=tooth thickness

x=loop designation

For the selected frame size, the corresponding shaft diameter can be determined from NEMA standard tables, then the core depth behind the deepest rotor slot can be calculated.

4.7.4 Rotor Resistances and Copper losses

Similar to the calculation of stator resistances, The rotor bar resistances can be determined by first determining the mean length per turn as

$$bl_x = 2 * L_a + \lambda_x \quad (4.78)$$

where

λ_x =the slot pitch corresponding to that loop

x =loop designation

Assuming that copper bars are to be used in this application, the resistivity for B187 copper is obtained from standard handbooks, [13], to be

$$\rho = 1.7504 \quad (4.79)$$

in $\mu\Omega\text{.cm}$ which is equivalent to $689 \mu\Omega\text{.inch}$. Therefore, the individual rotor bar resistances can be calculated as

$$r_x = \frac{bl_x * \rho}{dia_x^2} \quad (4.80)$$

Similarly, the end-ring resistance can be calculated in same manner, except in this case, the resistances will be for sub-segments of the end-ring. The total end-ring resistance will be the sum of all the sub-segments resistances. This method was employed in order to calculate the copper losses in these sub-segments individually, since they carry different current levels as shown above. Refer to Appendix-X for the sub-segment resistances calculation formulas.

The rotor-bar copper losses are calculated based on the above resistances and the rms currents

$$cl_x = nst * I_x^2 * r_x \quad (4.81)$$

and similarly the losses in the end ring

$$I_x = nst * I_x^2 * rsub_x \quad (4.82)$$

The total rotor copper losses is the sum of the above two losses.

4.7.5 Flux profile and Iron losses

The total flux crossing the air-gap and entering the rotor may be assumed to be the total flux due to the 6-pole winding plus that of the 2-pole winding.

$$\Phi_r = \Phi_6 * P_6 + \Phi_2 * P_2 \quad (4.83)$$

From this the flux densities in both the teeth and the core behind the deepest slot can be calculated in the same way as that of the stator. The core losses can be calculated by first obtaining the iron weights then estimating the watts per pound for the flux densities calculated above from established graphs, then scaling these values to be compatible with rotor frequency which is 15-Hz. These losses are expected to be very small due to the low frequency and flux densities.

The rotor teeth weight

$$mtr = .28 * wtr * L_a * (3 * dsu + 2 * dsv + 2 * dsw + 2 * dsx + dsy) * 4 \quad (4.84)$$

Refer to fig 4.13 for illustrations. Similarly, the core weight can be calculated in the same way while accounting for the shaft and any vents holes..

4.7.6 Calculated efficiency

When the BDFM is operating at full load speed, the 2-pole winding excitation is almost dc and iron losses are zero. Therefore the total machine losses at full load will be the sum of the 6-pole winding total losses plus the 2-pole winding copper losses and the rotor losses.

$$m_l = w_l 6 + w_{cu} 2 + w_l r \quad (4.85)$$

The efficiency if the machine can be calculated as

$$\eta = \frac{746 * HP}{746 * HP + m_l} \quad (4.86)$$

This value may be less than what was assumed in the beginning of the design since various assumptions and approximation were required during the design process. Another note is that all stator loss calculations were made at the equivalent induction machine windings ratings (currents, voltages, speeds). These values are expected to change when operating as a BDFM. The stator current will drop therefore reducing copper losses which should improve the calculated efficiency.

4.8 Practical Design

The previous sections described the ideal design process of the BDFM, from which the machine physical dimensions and slot specifics were obtained. Hence a

resulting product may not be cost effective. Therefore, such design procedure can be used as a guide for future special purposes BDFM applications.

In a practical design, the physical dimensions are known quantities beforehand and are dependent on the frame size utilized. For this application NEMA frame size-445 was selected due to availability and compatibility with the existing drive frame size. This fixes the outside diameter to a known value. Various lamination configurations, corresponding to different ratings requirements, with various slot widths, slot depths, bore diameters and lamination stack lengths can be accommodated in this frame.

To accommodate the two BDFM windings, a lamination configuration corresponding to an induction machine which is one standard rating (75-hp) higher than the proposed BDFM rating (60-hp) was selected. In addition, 72 semi-closed parallel teeth slots were selected. Therefore, the stator bore, slot area and tooth width are known quantities while the axial length can vary up to an upper limit. With these variables known, and for the winding ratings described in Section 4.4, the same design procedure as described in Sections 4.5 to 4.8 were followed with minor differences.

The air-gap flux densities for both windings are now calculated from equation-4.35 rather than assumed. For a suitable electric loading, obtained from fig 4.5 corresponding to the winding rating, the number of conductors per slot and per phase are calculated as was done in the ideal design. This in turn will lead to the calculation of the air-gap flux per pole and the air-gap flux density can then be calculated. These two densities should be comparable and any discrepancies are due to approximations in electric loadings and slot conductors.

The number and sizes of conductors to be used in this design are calculated in a similar fashion as previously discussed. However; since the actual slot dimensions

are available, a better prediction of the compatibility of the available slot area with the number and sizes of conductors used are obtained. This was done by calculating the actual slot area then comparing it to the total area of all conductors of both windings when at most a 76% fill factor was assumed. Refer to fig 4.14 below and the design spreadsheet for the details.

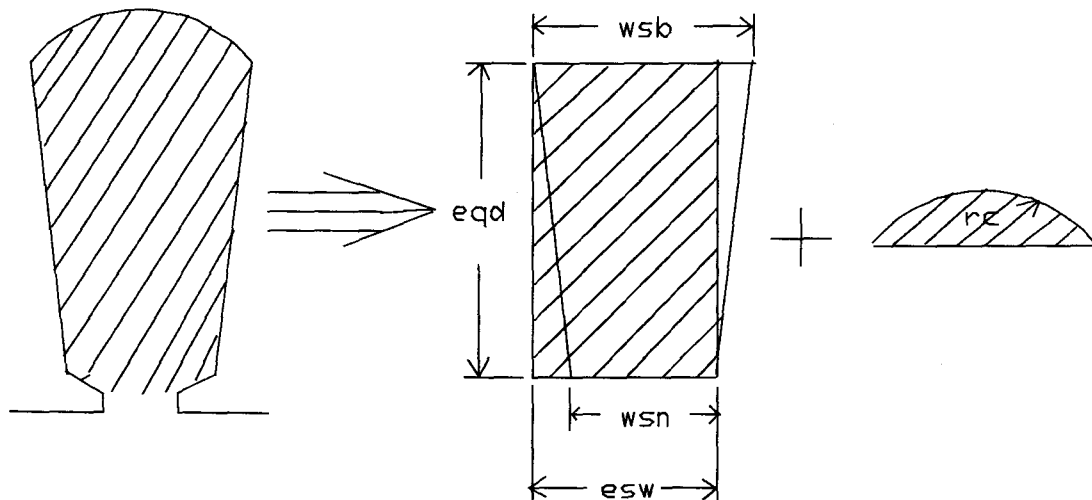


Figure 4.14 Slot area equivalent

4.9 Design Sheets and Their Layouts

As mentioned above, the design processes were carried out utilizing spreadsheet programming. The spreadsheet programming is the most suitable tool for this process since a lot of modifications and fine tuning of the design parameters are required.

Two design spreadsheets are provided in this document, one for the ideal design (BDFMID.XLS) and another one for the practical design (BDFMPD.XLS).

Each spreadsheet consist of 24-columns divided into 4, 6-columns sections corresponding to 6-pole design, 2-pole design, common design and rotor design respectively. Each section constitutes an item number, variable description, variable symbol, formula used, the corresponding value and a remark column.

The design sheets include two important features which need to be reckoned with by future users. The first one deals with variables the values of which are either known, to be approximated or assumed. These variables are then labeled as design inputs and designer must update them every time design parameters changed. It is important to note though, that not all variables with "input" label need to be updated each time a design parameter is changed. Instead only relevant ones need to be updated. The second feature are built in checking flags which monitor critical design variables and warn the user of possible design faults. These flags include: number of conductors selection; slot depth; slot area sufficiency to accommodated design conductors; current densities limits; flux densities limits. Fig-4.15 below is shown here to serve as an illustrative guidance for future users of the spreadsheet.

6-pole design	2-pole design	common calculations	rotor design
------------------	------------------	------------------------	-----------------

Figure 4.15 Design spreadsheets layouts

5. Conclusion and Recommendation

The procedures for the detail design of the BDFM were presented in this thesis. Two forms of design were considered. An ideal design, where the physical dimensions, slot details and conductors specifics were determined based on conservative assumptions of the machine loadings. The second form involves designing the BDFM, by determining conductor details and the associated machine loadings, based on the knowledge of the machine physical dimensions and slot details. In both cases a detailed "walk-through" example was employed by performing the design process to satisfy the proposed 60-hp pump drive. The new drive required performance was set by the existing drive performance and plant operational personnel preferences. This dictated the study of the existing drive system and the analysis of its performance.

It is important to note that this design procedure should be regarded as the first step in standardizing the manufacturing process of this machine. The design was limited to the BDFM 2-pole/6-pole stator winding configuration, which is one form of possibly many BDFM winding configurations. Should it become necessary to design such winding configurations, it will be necessary to modify the design spreadsheets to reflect these new changes. The most apparent changes would occur in the rotor number of nests which is dependant on the power and control windings pole-pairs numbers, and which in turn would affect the stator/rotor slot combination allowed.

The numbers of stator and rotor slots chosen in this design were intended to be viewed as a guide. Future users of the design sheets must select the slot combinations suitable for the particular application. However, it is known that better induction machine performance were obtained when the difference between stator and rotor slots is within 15% to 30%.

So for this application it is recommended that for the 72-stator slots, a 56-rotor slots, which is recommended as per Appendix-VII table, shall be used. This also provides a better copper to iron ratio in the rotor.

This design procedure can be considered as a link in the BDFM program completion. Other links involve the dynamic modelling and the steady state simulation program which are currently available. For successful use of these design sheets and an optimum utilization of the existing BDFM program tools, it is highly recommended that the general BDFM simulation program, which can provide machine variables (inductances, currents, voltages,...), be completed as soon as possible. This program is essential to the proper design and sizing of rotor bars capable of handling the specific application ratings. In addition and based on simulation results, fine tuning can be made to the design sheet to obtain better results before commencing the construction stage.

Two features, the input statement and the checking flags, were included in the design spreadsheets. Expansion of these features to be more specific in the case of the input statements, and to increase the number of interlock flags is recommended. Such addition may enhance the use of these design sheets. It is recommended that the standard values in the flag fields, which compares a design value to an equivalent allowable value, be up to the latest industrial standards in order for the design to be current.

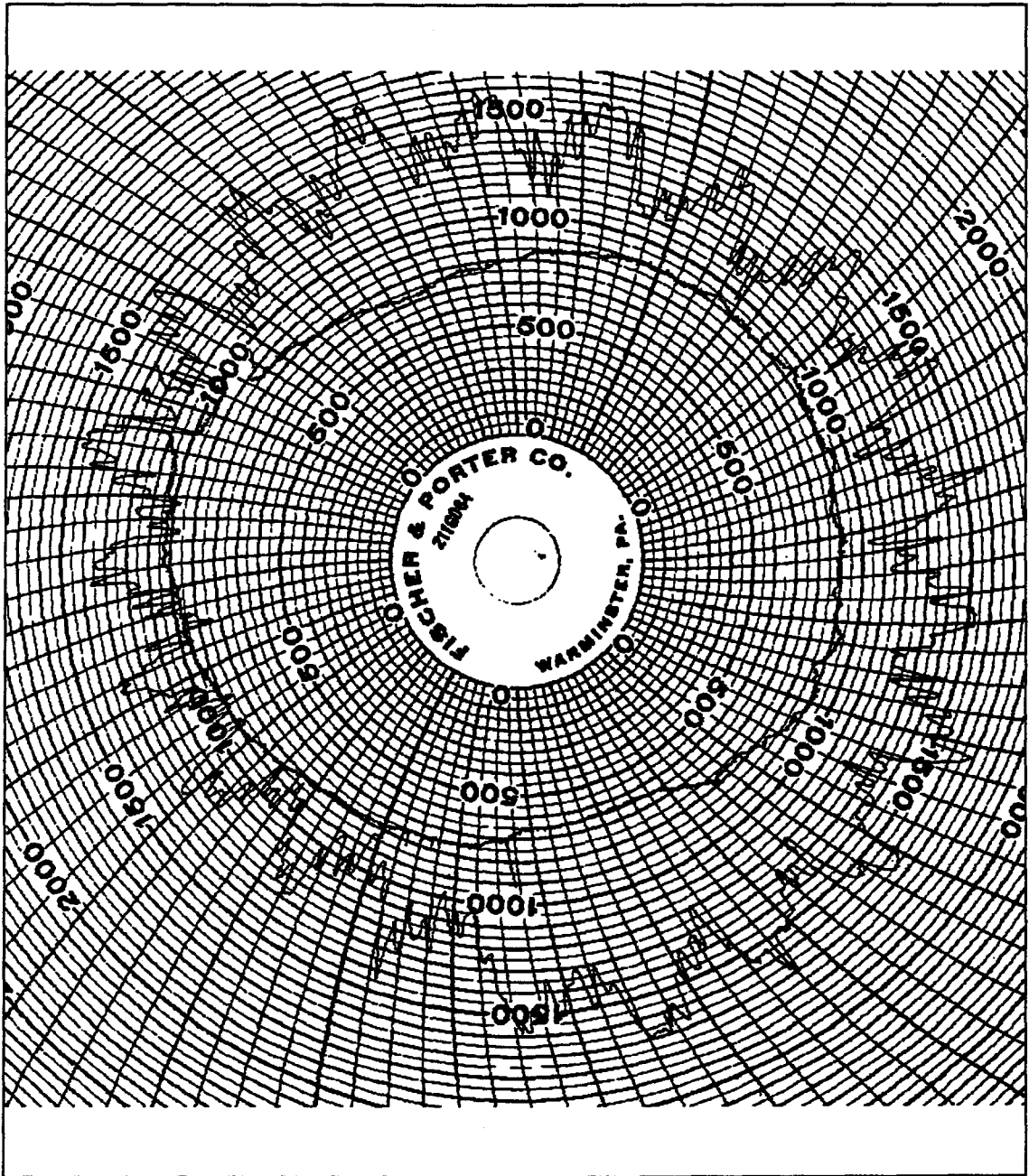
6. Bibliography

1. A. Wallace, R. Spee and H. Lauw, "The potential of Brushless Doubly Fed Machines for Adjustable Speed Drives," Proceedings, IEEE IAS Pulp and Paper Industry Annual Meeting, pp 45-50, June 1990.
2. A. Wallace, R. Spee and H. Lauw, "Dynamic Modelling of Brushless Doubly Fed Machines for Adjustable Speed Drives," Proceedings, IEEE IAS Annual Meeting, pp 329-334, October 1989.
3. Wallace, R. Spee and H. Lauw, " Performance simulation of Brushless Doubly Fed Adjustable Speed Drives," Proceedings, IEEE IAS Annual Meeting, pp 738-743, 1989.
4. R. Li, A. Wallace and R. Spee, "Two-axis Model Developement of Cage-Rotor Brushless Doubly-Fed Machines," Transactions IEEE PES, pp 453-460, march 1991.
5. R. Li, A. Wallace and R. Spee, "Dynamic Simulation of Brushless Doubly-Fed Machines," Transactions IEEE PES, pp 445-452, march 1991.
6. M. A. Salim and R. Spee, "High Frequency Cage Rotor Designs," IEEE IAS 1992
7. G.C. Alexander, R.Spee and A. K. Wallace, "Phase 3 of Brushless Doubly-Fed Machine System Development Program," Technical report prepared for BPA, EPRI, PSP&L.
8. M. G. Say, "The Performance and Design of Alternating Current Machines,"

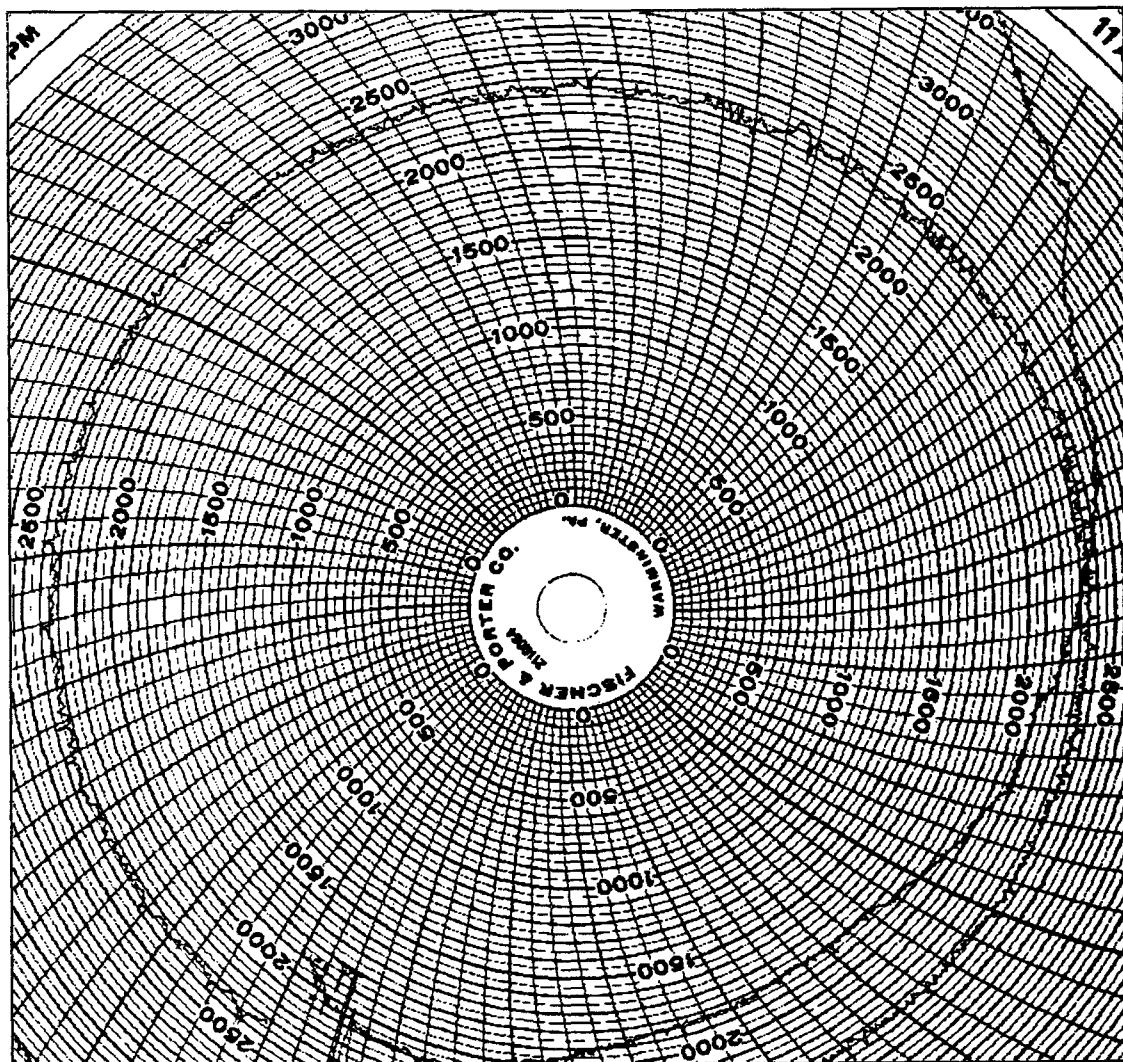
- Pitman and Sons, 1961.
9. S. Heller, " Multispeed and Standard Squirrel Cage Motors," Volume-1, Datarul, 1984.
 10. A. Wallace, P. Rochelle and R. Spee, "Rotor Modelling and Development for Brushless Doubly-Fed Machines," Int'l Conf. on Electric Machines, 1990
 11. A. Still and C. Siskind, "Elements of Electrical Machines Design," McGraw Hill, 1954.A.
 12. J. H. Khulmann, "Design of Electric Apparatus," Wiley and Sons, 1950..E.
 - 13 D. Fink and H. Beaty, "Standard Handbook for Electrical Engineers," 12th Eddition, McGraw Hill, 1987.
 14. E. Levi, "Polyphase Motors," Wiley and Sons, 1984.
 15. F. Creedy, "Some development in multi-speed cascade induction motors," Juornal Institution of Electrical Engineers, London, vol. 59, pp 511-521, 1921.

APPENDICES

Appendix-I; Pump Station Flow Chart, Irregular Flow



Appendix-II: Pump Station Flow Chart, Steady Flow



MEASUREMENTS: ROTOR VARIABLES
 ORIGINAL FILE NAME: RT701.WK1
 TEST SPEED: 700 RPM
 NEW FILE NAME: RT701M.XLS

TIME sec	Meter #	0001	0002		VOLTS AN VOLT	VOLTS BN VOLT	VOLTS CN VOLT	AMPS A AMP	AMPS B AMP	AMPS C AMP	K. WATT KW	K. VAR KVAR	K. VA KVA	P.F. %	FREQ. Hz	FLOW MG/D
	Desgn. Unit	speed volt	speed rpm	INST												
	DATE	POLL TIME	INST	INST	INST	INST	INST	INST	INST	INST	INST	INST	INST	INST	INST	INST
0	08-11-93	06:10:21	2.56	681.66	47	49	48	31	30	43	1.7	0	4.9	0	13.85	1.20987
17	08-11-93	06:10:38	2.58	686.98	46	48	48	34	31	44	1.8	0	5.2	0	14.28	1.11719
34	08-11-93	06:10:54	2.56	681.66	49	50	49	31	31	44	1.7	0	5.3	0	14.43	1.05533
51	08-11-93	06:11:05	2.55	678.99	49	51	48	30	32	43	1.7	0	5.2	0	14.48	1.01044
68	08-11-93	06:11:21	2.66	708.28	48	50	49	31	32	42	1.7	0	5.5	0	14.35	0.9673
85	08-11-93	06:11:36	2.64	702.96	44	43	40	33	36	41	1	0	4.5	0	12.85	0.931259
102	08-11-93	06:11:46	2.63	700.30	45	45	43	32	33	43	1.5	0	5.1	0	12.85	0.898575
119	08-11-93	06:11:56	2.65	705.62	42	42	40	33	34	41	1.1	0	4.2	0	12.79	0.882446
136	08-11-93	06:12:07	2.65	705.62	45	46	44	32	34	43	1.9	0	5.2	0	13.18	0.909683
153	08-11-93	06:12:22	2.63	700.30	43	44	43	31	32	44	1.5	0	4.8	0	12.63	0.931168
170	08-11-93	06:12:37	2.61	694.97	42	44	41	33	34	42	1.1	0	4.5	0	12.89	0.986786
187	08-11-93	06:12:52	2.61	694.97	44	45	44	33	33	42	1	0	4.6	0	13.37	1.01556
204	08-11-93	06:13:03	2.6	692.31	45	47	46	33	32	43	1.9	0	5.2	0	13.73	1.08591
	AVERAGE		2.61	694.97	45.31	46.46	44.85	32.08	32.62	42.69	1.51	0.00	4.94	0.00	13.51	1.00

**STATOR VARIABLES
OVER SPEED RANGE**

dc volts volt	SPEED rpm	VOLTS AN VOLT	VOLTS BN VOLT	VOLTS CN VOLT	AMPS A AMP	AMPS B AMP	AMPS C AMP	K. WATT KW	K. VAR KVAR	K. VA KVA	P.F. %	FREQ. Hz	FLOW MGPD
2.61	694.97	269.69	235.08	268.54	68.19	66.79	67.62	26.66	44.95	52.34	0.51	60.00	0.99
2.74	730.75	269.38	235.31	267.94	69.51	68.21	69.03	29.06	44.75	53.44	0.54	60.00	2.14
2.79	744.15	269.00	234.65	268.00	70.71	68.61	70.39	30.38	44.70	54.12	0.56	60.00	2.34
2.86	762.20	269.31	235.50	267.88	72.92	70.41	72.33	32.88	44.90	55.72	0.59	60.00	3.71
2.95	784.50	268.94	234.81	267.00	75.09	72.24	74.34	35.42	44.71	57.10	0.62	60.00	4.54
3.02	802.91	272.31	238.92	270.69	78.46	75.09	78.12	37.76	47.31	60.59	0.62	60.00	4.96
3.11	826.85	272.06	239.94	270.12	80.42	77.33	80.05	40.56	47.13	62.23	0.65	60.00	5.59
3.26	866.93	272.11	240.63	270.42	83.32	80.73	84.07	44.88	46.97	65.00	0.69	60.00	6.61

ROTOR VARIABLES OVER SPEED RANGE													
dc volts volt	SPEED rpm	VOLTS AN VOLT	VOLTS RN VOLT	VOLTS CN VOLT	AMPS A AMP	AMPS B AMP	AMPS C AMP	K. WATT KW	K. VAR KVAR	K. VA KVA	P.F. %	FREQ. Hz	FLOW MG/D
2.61	695.24	45.80	46.80	45.20	31.80	32.50	42.80	1.56	0.00	4.99	0.00	13.57	0.99
2.74	730.75	36.13	37.50	35.94	35.50	35.94	45.81	1.13	0.00	4.38	-0.30	10.87	2.14
2.79	744.15	33.76	33.82	32.82	37.35	38.24	46.53	1.22	0.00	4.06	0.19	6.40	2.34
2.86	762.20	27.69	28.38	27.19	40.50	42.69	48.88	0.95	-0.71	3.65	0.03	0.00	3.71
2.95	784.50	22.25	23.19	21.94	45.38	47.00	50.38	0.84	0.28	3.29	0.62	0.00	4.54
3.02	802.91	18.08	18.54	17.92	47.85	49.46	51.23	0.69	0.00	2.78	0.46	0.00	4.96
3.11	826.85	12.06	12.18	12.00	52.82	52.53	49.24	0.31	0.00	1.95	0.16	0.00	5.59
3.26	866.93	4.21	4.58	4.32	41.63	41.68	38.21	-0.05	0.00	0.59	-0.25	0.00	6.61

EXISTING DRIVE PERFORMANCE ANALYSIS TABLE

SPEED rpm	SPEED %	SLIP	STR Vph VOLT	STR Iph AMP	INPT PWR KW	STR K. VAR KVAR	STR K. VA KVA	P.F.	RTR Vph VOLT	RTR Iph AMP	RTR X R LOSS KW	RTR X RES OHMS
694.97	77.22	0.23	258.27	67.54	26.66	44.95	52.34	0.51	45.94	36.05	4.97	1.27
730.75	81.19	0.19	258.02	68.92	29.06	44.75	53.44	0.54	36.53	39.37	4.31	0.93
744.15	82.68	0.17	257.71	69.91	30.38	44.70	54.12	0.56	33.47	40.92	4.11	0.82
761.85	84.65	0.15	258.00	71.85	32.82	44.90	55.68	0.59	27.75	44.16	3.68	0.63
784.50	87.17	0.13	257.39	73.90	35.42	44.71	57.10	0.62	22.46	47.63	3.21	0.47
802.91	89.21	0.11	261.09	77.24	37.76	47.31	60.59	0.62	18.18	49.53	2.70	0.37
826.85	91.87	0.08	261.12	79.28	40.56	47.13	62.23	0.65	12.08	51.56	1.87	0.23
866.93	96.33	0.04	261.45	82.72	44.88	46.97	65.00	0.69	4.37	54.30	0.71	0.08

SPEED rad/sec	P.F. %	STR INPUT KW	STR Cu LOSS KW	IRON LOSS KW	RTR X R LOSS KW	RTR Cu LOSS KW	F & W PWR KW	OTPT PWR KW	EFF %	TORQUE NM	FLOW MGPD	WELL LVL FT
72.78	50.89	26.66	1.09	1.12	4.97	0.37	0.67	18.44	69.16	253.40	0.99	193.45
76.52	54.33	29.06	1.14	1.12	4.31	0.44	0.73	21.32	73.35	278.55	2.14	193.25
77.93	56.08	30.38	1.17	1.12	4.11	0.48	0.76	22.74	74.85	291.86	2.34	192.95
79.78	58.88	32.82	1.24	1.12	3.68	0.56	0.82	25.41	77.41	318.45	3.70	192.71
82.15	61.99	35.42	1.31	1.12	3.21	0.65	0.89	28.25	79.75	343.86	4.54	192.50
84.08	62.29	37.76	1.43	1.12	2.70	0.70	0.94	30.86	81.73	367.05	4.96	192.40
86.59	65.14	40.56	1.51	1.12	1.87	0.76	1.01	34.29	84.54	396.04	5.59	192.30
90.78	68.98	44.88	1.64	1.12	0.71	0.84	1.12	39.44	87.88	434.41	6.61	192.10

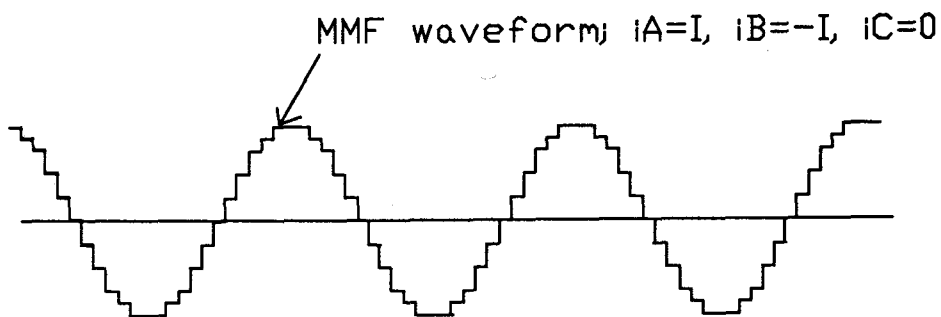
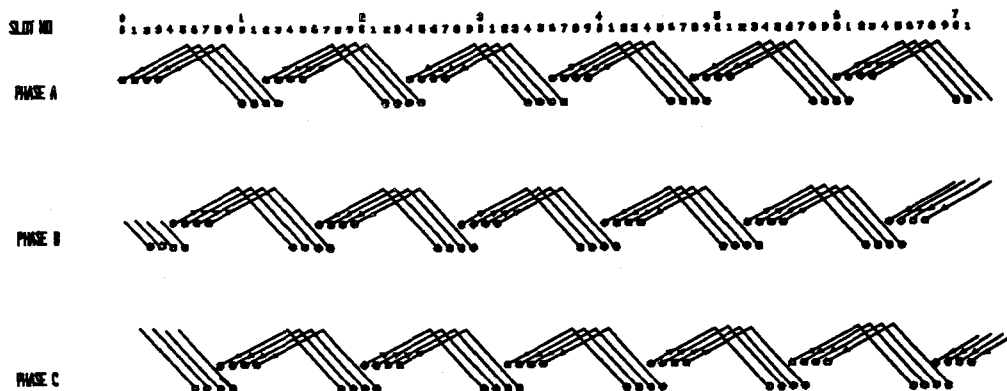
STATOR WINDING RESISTANCE $r_s=.08$
ROTOR WINDING RESISTANCE $r_r=.095$
IRON LOSS= $.025 * 44.88KW$
FRICTION AND WINDAGE LOSS = $.025 * INPUT POWER$
TORQUE=OUTPUT POWER (watts)/SPEED(rad/sec)

Appendix-VII: Slot Combination Table

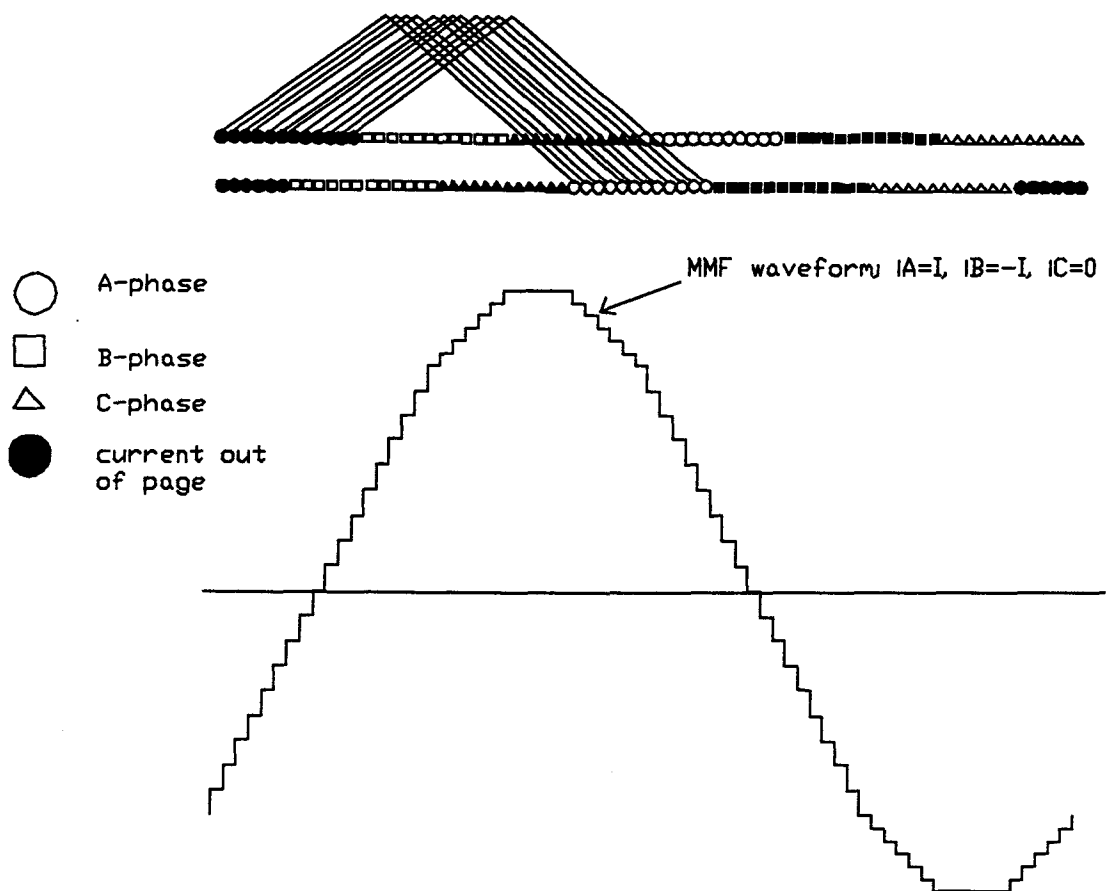
	ns	72	72	72	72	72	72	72	72	72	72	72	72	72	54	54	54	54	54	54	54	54	54	54	54	54	54	54	36	36	36	36	36	36	36	36	36	36	36	36	36	36	36	
	nr	20	24	28	32	36	40	44	48	52	56	60	64	68	20	24	28	32	36	40	44	48	52	56	60	64	68	20	24	28	32	36	40	44	48	52	56	60	64	68				
	pole	6																																										
condition																																												
1	1																																											
2	2																																											
p	6																																											
p+1	7																																											
p+2	8																																											
2p	12																																											
3p	18																																											
5p	30																																											
	ns	72	72	72	72	72	72	72	72	72	72	72	72	72	54	54	54	54	54	54	54	54	54	54	54	54	54	54	36	36	36	36	36	36	36	36	36	36	36	36	36	36	36	36
	nr	20	24	28	32	36	40	44	48	52	56	60	64	68	20	24	28	32	36	40	44	48	52	56	60	64	68	20	24	28	32	36	40	44	48	52	56	60	64	68				
	pole	2																																										
condition																																												
1	1																																											
2	2																																											
p	2																																											
p+1	3																																											
p+2	4																																											
2p	4																																											
3p	6																																											
5p	10																																											
6p	12																																											
9p	18																																											
12p	24																																											

Stator/Rotor Slot Combination Schedule For ns=72,54,36; nr=from 20 to 68
X; Indicate a non-recommended combination

Appendix-VIII; Winding Layout and Corresponding MMF
Waveform, 6-Pole



Appendix-IX; Winding Layout and Corresponding MMF Waveform, 2-Pole



Appendix-X; BDFM Ideal Design Spreadsheet

BDFM DESIGN; 6-POLE WINDING

Item	DESCRIPTION	sym	FORMULA	VALUE	REMARKS
1	motor ratings (Hp)	Hp	design parameter	80.00	*** input***
2	# of phases	m	3.00	*** input***
3	rms line voltage (volts)	Vl	460.00	*** input***
4	frequency (Hz)	fs	60.00	*** input***
5	synchronous speed (rpm)	N	1200.00	*** input***
6	# of poles	p	given; =120*fs/N	6.00	
7	full load power factor	pf	design parameter	0.91	*** input***
8	full load efficiency	h	0.92	*** input***
9	gap flux density in main pole (lines/sqr in)	Bg	assumed	2.60E-04	*** input***
10	elec. specific loading (amper-coad./in^2)	Q	determined from given graphs	675.00	*** input***
11	total number of stator slots	ns	given	72.00	*** input***
12	number of slots per pole per phase	nspp	nspp=ns/m*p	4.00	
13	# of slots per pole	nsp	such that # of slots/pole/phase >=2	12.00	
14	# of slots per phase	nsp	nsp=nspp*p	24.00	
15	# of electrical degrees between slots	β	beta=180*p/ns	15.00	
16 in rad	β	in rad=beta(deg)*p/180	0.26	
17	distribution factor	fd	fd=sin(nsp*beta/2)/nsp*sin(beta/2)	0.96	
18	coil span in electrical degrees	gamma	obtained from winding schematics	150.00	*** input***
19	coil pitch (pu)	cp	assumed for the design to be 5/6	0.8333333333	*** input***
20	pitch factor	fp	fp=sin(gamma/2); 2-for double layer winding	0.97	gamma converted to radian
21	winding factor	d	d=fd*fp	0.93	typical values between (.90 to .96)
22	stator inside diameter and length (in^3)	D^2*La	(4.87*Hp*10^11)/(Bg*Q*d*N*eta*pf)	1996.37	
23	phase voltage (volts)	E	Vl/sqrt(3)	265.58	
24	full load phase current (amps)	Ip	746*Hp/(3*E*eta*pf)	89.47	
25					
26	D, in DETERMINATION
27					
28	the calculated axial length	La	La=the cubic root((4*pi*D^2*La)/p^2)	8.87	based on square polar law
29	stator inside diameter (in); approximated	D'	D'=sqrt(D^2*La/La)	15.01	square polar principle
30	stator inside diameter (in); approximated	D	selected	15.00	*** input***
31	pole pitch; designed (in)	tau	D*pi/cp/p	6.54	design value used for calculations
32	stator gross core length (in), axial length	La	d^2*La/D^2	8.87
33					
34					
35	DESIGN DIAMETER	D		15.00	**** must update if different than above ***

36	DESIGN LENGTH	la		8.90	*** must update if different than above***
37					
38	slot pitch (in)	λ	$\lambda = \text{lamda} = \tau / \# \text{ of slots per pole}$	0.55	calculated at air-gap
39					
40	# of stator conductors per slot calculated	Cs'	$Cs' = Q * \text{lamda} / p$	4.11	calculated at mean length
41	selected	Cs	# of cond./slot must be even # for dbl lyr wding	4.00	*** input***
42	# of stator conductors per phase	Z	$Z = Cs * n * s * p$	96.00	
43					
44	air-gap flux per pole (lines "maxwells")	ϕ	$\text{phee} = E * 10^8 / (2.22 * d * Z)$	2.25E+06	
45	corrected air-gap density (lines/in^2)	Bg	$Bg = \text{phee} / \tau * la$	38544.91	
46	maximum air gap density (lines/in^2)	Bgm	$Bgm = \text{sqrt}(2) * Bg$	54510.73	
47	maximum apparent flux density (lines/sqr in)	Btm'	assume to be 85000	85000.00	*** input *** typical
48	tooth width selected, (in)	wt'	$wt' = Bgm * \text{lamda} / Btm$	0.35	
49		wt	selected	0.34	
50	the slot width, (in)	ws	$ws = \text{lamda} - wt$	0.21	
51	maximum teeth density corrected, (lines/in^2)	Btm	$Btm = Btm' * wt' / wt$	87444.09	shall be made small enough to account for 2-pole
52					
53	current density; assumed, (amp/in^2)	Δ	assumed; between (3500 - 5000) amps/in^2	4500.00	*** input***
54	cond. cross sectional area, calculated (in^2)	ca'	$ca' = Ip / \text{delta}$	0.019882392	awg#6 area is .02061 in^2, .162 in dia
55	actual conductor diameter/thickness, (in)	dla	to fit the above calculated area	0.162	*** input ***
56	area, (in^2), (in)	ca	one awg#5 at .026 in^2	0.02061	*** input ***
57	substitute conductor area (in^2)	cas	one AWG#17 @ .001609	0.001609	*** input ***
58	substitute conductor diameter (in)	dias	one AWG#17 @ .04526	0.04526	*** input ***
59	# of stator substitute conductors per slot	Csa'	$Csa' = Cs * (ca / cas)$	51.23679304	Csa must be even for double layer winding
60		Csa	chosen so that it is even and satisfies ca'	64	*** input ***
61	# of conductors in parallel	pc	$pc = Csa / Cs$	16	FLAG: integer parallel conductors OK
62	current density, calculated, (amp/in^2)	Δ	$\text{delta} = Ip / (Csa * cas / Cs)$	3475.40	FLAG: CURRENT DENSITY LOW
63	CHECK IF # OF SUBSTITUTE CONDUCTORS SATISFIES ca'			"----->	FLAG: CALCULATED AREA SATISFIED
64					
65					
66					
67					
68					
69	thickness of insulation (in)	ti	$ti = 15 / 1000$	0.01	typical of now a days insulations, fixed
70	slot width available for wires, (in)	wsw	$wsw = ws - 2 * ti$	0.185415391	
71	number of cond. which can fit slot width	wsl	$wsl = \text{integer}(wsw / dias)$	4	
72	# of rows of wires in the slot	wr	$wr = csa / wsl$	16	
73	selected	wr		16	*** input ***
74	depth of wires stacked in the slot, (in)	wd	$wd = wr * dias$	0.72416	
75	double layer spacer	dls	$dls = 30 / 1000 "$	0.03	fixed
76	slot lining	ls	ls=insulation thickness	0.01	fixed

77	allowance for spaces between wires	all	$all=3/1000''$	0.03	fixed
78	slot depth of the 6-pole (in)	ds6	$ds6=wd+dl+ls+all$	0.79416	
79					
80					
81					
82	# of coils sides per slot	csps	csps=2; for double layer windings	2.00	*** Input ***
83	# of coil sides per phase	csph	$csph=nsp*csps$	48.00	
84	# of coils per phase	cph	$cph=csph/csps$	24.00	2-coil sides per coil
85	# of coil per pole per phase	cpph	$cpph=cph/p$	4.00	
86	# of conductors per coil side	cpcs	$cpcs=Cu/csps$	2.00	
87	# of turns per coil	Nc	$Nc=cpcs$	2.00	
88	# of turns per phase in series	Ns	$Ns=Nc*cph$	48.00	
89					
90					
91	coil thickness plus clearance between end coils(in)	d1	$d1=ws+s$	0.33	s was assumed to be .12
92	approximate angle of bend of end winding (rad)	alpha	$alpha=arcsin(d1/lambdam)$	0.64	
93	pole pitch at the mean of the slot (in)	taum	$taum=tau$; assumed for now	6.54	
94	end winding horizontal length of one end	2hw	$2hw=taum/cos(alpha)$	8.16	
95	overhang length	oh	assumed to be the size of the slot depth	1.65	
96	mean length per turn of stator winding	mlt	$mlt=2*la+4*oh+2*(2hw)$	48.72	
97	winding length per phase (ft)	wl	$wl=Ns*mlt/12$	162.87	
98	resistance per M ft of specified conductor	rs'	from NEC @ 75 deg C	5.06	*** Input ***
99	resistance per phase ohms	rs	$rs=wl*rs'/1000*pc$	0.051547356	resistance per 1000 ft given by AWG wire table
100					
101	IR drop per phase (volts)	IR	$IR=Ip*rs$	4.61	
102	total stator copper loss, 6-pole (Watts)	Wcu6	$Wcu6=3*Ip*IR$	1237.91	
103					
104	flux density in iron of stator lines/in ²	Bc'	assume 70000	70000.00	*** Input ***
105	flux in stator core/pole (lines)	pheec	assume to be half that of air gap	1.12E+06	
106	core depth behind slots; 6-pole (in)	crd'	$crd'=pheec/(la*Bc)$	1.80	
107	outside diameter, (in)	Do	$Do=2(crd+ds)+D$	21.91	calculated
108	outside diameter chosen	Do	select to suit a frame and avoid core saturation	22.00	*** Input *** chosen to fit frame designation G
109	core depth behind slots (in)	crd	$crd=(Do-2*ds-D)/2$	2.71	calculated
110	flux density in iron (lines/in ²)	Bc	$Bc=pheec/(la*crd)$	46616.91	
111					
112					
113					
114	weight of iron in stator core (lb)	mc	$mc=.28*pi*(Do-crd)*crd*la$	408.72	assuming .28lb/cubic in; for USS M-36
115	weight of iron in stator teeth (lb)	mt	$mt=.28*wt*ns*ds*la$	48.45	assuming uniform tooth width
116	watts per pound for core USS-M-36, 26 gage	wibc	obtained from graph @ Bc=60k lines/in ²	1.10	*** Input***
117	watts per pound per cycle for tooth	wibt	***** @ Bt=87k lines/in ²	2.10	*** Input***

BDFM DESIGN; 2-POLE WINDING

Item	DESCRIPTION	sym	FORMULA	VALUE	REMARKS
1	motor ratings (Hp)	Hp	known	90.00	*** Input***
2	# of phases	m	known	3.00	*** Input***
3	rms line voltage (volts)	Vl	known	1380.00	*** Input***
4	frequency (Hz)	fs	known	-60.00	*** Input***
5	synchronous speed (rpm)	N	known	-3600.00	*** Input***
6	# of poles	p	given; =120*fs/N	3.00	
7	full load power factor	pf	known	0.91	*** Input***
8	full load efficiency	η	known	0.93	*** Input***
9					
10	elec. specific loading (amper-cond./in ²)	Q	determined from given graphs	675.00	*** Input***
11	total number of stator slots	ns	given	72.00	*** Input*** (stator lamination design)
12	number of slots per pole per phase	nspp	nspp=ns/m*p	12.00	
13	# of slots per pole	nsp	nsp=ns/p	36.00	
14	# of slots per phase	nsph	spph=nspp*p	24.00	
15	# of electrical degrees between slots	β	beta=180°p/ns	5.00	
16 in rad	β	in rad=beta(deg)*pi/180	0.09	
17	distribution factor	fd	fd=sin(nspp*beta/2)/nsp*sin(beta/2)	0.96	
18	coil span in electrical degrees	gamma	obtained from winding schematics	150.00	*** Input***
19	coil pitch (pu)	cp	assumed for the design to be 5/6	0.833333333	*** Input***
20	pitch factor	fp	fp=sin(gamma/2); 2-for double layer winding	0.97	gamma converted to radian
21	winding factor	d	d=fd*fp	0.92	typical values between (.90 to .96)
22	gap flux density in main pole (lines/sqr in)	Bg	Bg=4.07*Hp*10 ⁻¹³ /(D ² *ta*Q*d*N*eta*pf)	-9.64E+03	based on dimensions found from frame maximum design
23					
24					
25	phase voltage (volts)	E	Vl/sqrt(3)	796.74	
26	full load phase current (amps)	Ip	746*Hp*eta/(3*E*pf)	28.71	note effect of efficiency compared to 4-pole
27					
28					
29					
30					
31	pole pitch; designed (in)	tau	D*pi*cp/p	19.60	design value
32					
33					
34					
35					

36					
37					
38	slot pitch (in)	λ	$\lambda = \tau / nsp$	0.54	calculated at the air-gap
39					
40	# of stator conductors per slot calculated	Cs'	$Cs' = Q' \lambda / lp$	12.00	calculated at mean length
41	selected	Cs	# of cond./slot must be even # for dbl lyr wndng	10.00	*** input ***
42	# of stator conductors per phase	Z	$Z = Cs' * nsp * p$	240.00	
43					
44	air-gap flux per pole (lines "maxwells")	ϕ	$\phi = E * 10^{-8} / (2.22 * d * r * Z)$	-2.70E+06	
45	corrected air-gap density (lines/in^2)	Bg	$Bg = \phi / \tau * la$	-15484.74	
46	maximum air gap density (lines/in^2)	Bgm	$Bgm = \sqrt{2} * Bg$	-21898.73	
47	surface area at air-gap	sag	$sag = \pi * D * La$	419.40	
48	teeth surface area	tsa	$tsa = wt * La * ns$	217.87	
49	tooth width	wt	selected	0.34	same as in the 6-pole
50	the slot width, (in)	ws	$ws = \lambda - wt$	0.21	same as in the 6-pole
51	maximum teeth density corrected, (lines/in^2)	Bitm	$Bitm = sag * Bgm / tsa$	-42154.96	
52					
53	current density; assumed, (amp/in^2)	Δ	assumed; between (2000 - 3000) amps/in^2	4500.00	*** input ***
54	cond. cross sectional area, calculated (in^2)	ca'	$ca' = lp / \delta$	0.006379265	awg#10 area is .00815 in^2, .1019 in dia
55	actual conductor diameter/thickness, (in)	dia	to fit the above calculated area	0.1019	*** input ***
56	area, (in^2), (in)	ca	one awg#5 at .026 in^2	0.00815	*** input ***
57	substitute conductor area (in^2)	cas	one AWG#17 @ .001609	0.001609	*** input ***
58	substitute conductor diameter (in)	dias	one AWG#17 @ .04526	0.04526	*** input ***
59	# of stator substitute conductors per slot	Csa'	$Csa' = Cs' * (ca / cas)$	50.65257924	Csa must be even for double layer winding
60	selected	Csa	chosen so that it is even and satisfies ca'	60	*** input ***
61	# of conductors in parallel	pc	$pc = Csa / Cs$	6	FLAG: Integer parallel conductors OK
62	current density, calculated, (amp/in^2)	Δ	$\delta = lp / (Csa * cas / Cs)$	2973.55	FLAG: CURRENT DENSITY LOW
63	CHECK IF # OF SUBSTITUTE CONDUCTORS SATISFIES ca'			"----->	FLAG: CALCULATED AREA SATISFIED
64					
65					
66					
67					
68					
69	thickness of insulation (in)	ti	$ti = 15 / 1000$	0.01	typical of now a days insulations, fixed
70	slot width available for wires, (in)	wsw	$wsw = ws - 2 * ti$	0.185415391	
71	number of cond. which can fit slot width	wni	$wni = \text{integer}(wsw / dias)$	4	
72	# of rows of wires in the slot	wr	$wr = csa / wni$	15	
73	selected	wr		15	*** input ***
74	depth of wires stacked in the slot, (in)	wd	$wd = wr * dias$	0.6789	
75	double layer spacer	dis	$dis = 30 / 1000$	0.03	fixed
76	slot lining	ls	ls=insulation thickness	0.01	fixed

77	allowance for spaces between wires	all	all=3/1000"	0.03	fixed
78	slot depth of the 6-pole (in)	ds2	ds2=wd+dls+ls+all	0.7489	
79					
80					
81					
82	# of coils sides per slot	csps	csps=2; for double layer windings	2.00	*** Input ***
83	# of coil sides per phase	csph	csph=nsph*csps	48.00	
84	# of coils per phase	cph	cph=csph/csps	24.00	2-coils sides per coil
85	# of coil per pole per phase	cpph	cpph=cph/p	12.00	
86	# of conductors per coil side	cpcs	cpcs=Cc/csps	5.00	
87	# of turns per coil	Nc	Nc=cpcs	5.00	
88	# of turns per phase in series	Ns	Ns=Nc*cph	120.00	
89					
90					
91	coil thickness plus clearance between end coils(in)	d1	d1=ws+s	0.33	s was assumed to be .12
92	approximate angle of bend of end winding (rad)	alpha	alpha=arcsin(d1/lambdam)	0.64	
93	pole pitch at the mean of the slot (in)	taum	taum=tau; assumed for now	19.60	
94	end winding horizontal length of one end	2hw	2hw=taum/cos(alpha)	24.45	
95	overhang length	oh	assumed to be the size of the slot depth	1.65	
96	mean length per turn of stator winding	mlt	mlt=2*ls+4*oh+2*(2hw)	73.30	
97	winding length per phase (ft)	wl	wl=Ns*mlt/12	733.00	
98	resistance per M ft of specified conductor	rs'	from NEC @ 75 deg C	5.06	*** Input ***
99	resistance per phase ohms	rs	rs=wl*rs'/1000*pc	6.618655414	resistance per 1000 ft given by AWG wire table
100					
101	IR drop per phase (volts)	IR	IR=lp*rs	17.76	
102	total stator copper loss, 6-pole (Watts)	Wcu6	Wcu6=3*lp*IR	1529.45	
103					
104	flux density in iron of stator lines/in^2	Bc'	assume 70000	70000.00	*** Input ***
105	flux in stator core/pole (lines)	pheec	assume to be half that of air gap	-1.35E+06	
106	core depth behind slots; 6-pole (in)	crd'	crd'=pheec/(ls*Bc)	2.17	
107	outside diameter, (in)	Do	Do=2(crd'+ds)+D	22.64	calculated
108	outside diameter chosen	Do	select to suit a frame and avoid core saturation	22.00	*** Input *** chosen to fit frame designation G
109	core depth behind slots; 6-pole (in)	crd	crd=(Do-2*ds-D)/2	2.75	calculated
110	flux density in iron (lines/in^2)	Bc	Bc=pheec/(ls*crd)	-55159.92	
111					
112					
113					
114	weight of iron in stator core (lb)	mc	mc=.28*pi*(Do-crd)*crd*ls	414.58	assuming .28lb/cubic in; for USS M-36
115	weight of iron in stator teeth (lb)	mt	mt=.28*wt*ns*ds*ls	45.69	assuming uniform tooth width
116	watts per pound for core USS-M-36, 26 gage	wbfc	obtained from graph @ Bc=70k lines/in^2	1.50	*** Input***
117	watts per pound per cycle for tooth	wibt	***** @ Bt=42k lines/in^2	0.60	*** Input***

COMMON CALCULATIONS FOR BOTH WINDINGS					
Item	description	sym	formula	value	remark
1					
2	TOTAL STATOR LOSSES				
3					
4	total stator copper loss (watts)	wcu1	$wcu1 = wcu16 + wcu12$	71237.91	
5	total stator iron loss (watts)	wsll	$wsll = wsll6$	551.33	
6	total stator loss (watts)	wsl	$wsl = wcu1 + wsll$	71789.24	account for both windings
7					
8					
9	MAX. INSTANTANEOUS TEETH FLUX DENSITY				
10					
11					
12					
13	maximum instantaneous flux density	Btm	$Btm = Btm6 + Btm2$	129599.05	FLAG; HIGH TEETH FLUX DENSITY
14	maximum instantaneous core flux density	Bcm	$Bcm = Bc6 + abs(Bc2)$	101776.83	FLAG; FLUX DENSITY WITHIN RANGE
15					
16					
17	CALCULATED SLOT DEPTH AND CONDUCTORS AREA				
18					
19					
20					
21	wedge thickness (in)	wdt	$wdt = 30/1000$	0.05	***input***
22	tooth thickness (in)	tt	assumed	0.03	***input***
23	spacer between the two windings (in)	s62	may not be required	0.03	***input***
24	total slot depth, (in)	ds	$ds = ds6 + ds2 + wdt + tt$	1.65	
25					
26	total # of conductors in the slot	c	$c = Cas6 + Cas2$	124.00	
27	area of conductors	cas	from the 2/6-pole designs	0.001609	
28	total area required by all conductors in the slot	cat	$cat = cas * c$	0.20	
29					
30	REQUIRED SLOT AREA CALCULATION				
31					
32					
33					
34	fill factor	ff	assume 76%	0.76	***input***
35	required slot area (in ²)	rsa	$rsa = 1.24 * cat$	0.25	
36	slot arc radius (in)	rc	$rc = .2171$, assumed	0.22	***input***, typical

37	slot depth excluding the arc and area below wedge	eqd	$eqd = ds - wdt - H - rc$	1.35596	
38	equivalent slot width (in)	esw	$esw = (rsa - pi * rc^2 * 2/2) / eqd$	0.13	
39					
40	SUMMARY SHEET				
41					
42					
43					
44					
45	6-POLE WINDING				
46					
47					
48	type of winding used		double layer winding		
49	wire size used		# 17 AWG		
50	fractional pitch	fp	assumed for this design	0.83	5/6 th fractional pitch used
51	total number of conductors used/slot	Cas6		64.00	
52	number of parallel conductors	pc6		16.00	
53	number of coils per pole per phase	cpph		4.00	
54	number of turns per coil	Nc		2.00	
55	number of turns/phase	Ns6		48.00	
56					
57	2-POLE WINDING				
58					
59					
60	type of winding used		double layer winding		
61	wire size used		# 17 AWG		
62	fractional pitch	fp	assumed	0.83	5/6 th fractional pitch used
63	total number of conductors used/slot	Cas2		60.00	
64	number of parallel conductors	pc2		6.00	
65	number of coils per pole per phase	cpph		12.00	
66	number of turns per coil	Nc		5.00	
67	number of turns	NS2		120.00	
68					
69					
70	DESIGN DIAMETER (in), (m)	D	(in), (m)	15	0.381
71	DESIGN LENGTH (in), (m)	la	(in), (m)	8.9	0.22606
72	DESIGN AIR-GAP LENGTH (in), (m)	Lg	$Lg = .125 - (10.17 / (D + 90))$	0.028142857	0.000714829
73	DESIGN AIR-GAP LENGTH (mm)			0.714828571	
74					
75					
76					
77					

78		SIMULATION PROGRAM			
79		REQUIRED DATA			
80					
81					
82	stack length (m)	La	calculated previously	0.22606	
83	machine inside diameter (m)	D	0.381	
84	air-gap radial length (m)	lg	0.000714629	
85	resistivity of rotor bars materials (ohms-cm)	sigma	1.75	***input***
86	assumed rotor bar area (c. mills)	car	from tables for AWG# 1	83690.00	
87					
88					
89	# of turns per coil (power winding)	Np		2.00	
90	winding length per coil (ft)	mltcp	$mltcp = ml \cdot Np / 12$	6.79	
91	coil resistance ohms	rcp	$rcp = rs \cdot mltcp / 1000$	0.055035474	
92					
93	# of turns per coil (control winding)	Nc		5.00	
94	winding length per coil ft	mltcc	$mltcc = ml \cdot Nc / 12$	30.54	
95	coil resistance ohms	rcc	$rcc = rs \cdot mltcc / 1000$	0.671920375	
96					
97					
98	number of rotor slots	nr		40.00	
99	number of nests	nst	known for BDFM	4.00	
100	rotor turns/loop	Nr	1.00	*** input***
101	rotor loops per nest	nstl		5.00	

BDFM ROTOR DESIGN					
item	description	sym	formula	value	remark
1					
2	number of rotor poles	pr	constant for bdfm	4.00	*** Input ***
3	air-gap radial length (in)	lg	$lg = 125 \cdot (10.17/D + 90)$	0.03	
4	rotor diameter (in)	Dr	$Dr = D - 2 \cdot lg$	14.94	
5	number of rotor slots	nr	chosen to avoid cogging, cusping & noise	40.00	*** Input ***
6	number of nests	nst	known for BDFM	4.00	*** Input ***
7	number of slots per pole	nrp	$nrp = nr/pr$	10.00	
8	rotor slot pitch in degrees	lamdar'	$lamdar' = 360/nr$	9.00	
9	rotor slot pitch (in)	lamdar	$lamdar = lamdar' \cdot \pi \cdot Dr / 360$	1.17	
10	pole pitch (in)	taur	$taur = \pi \cdot Dr / pr$	11.74	
11					
12					
13					
14					
15					
16					
17	rotor slot width (in)	wsr'	assume a size to fit AWG #1 diameter	0.30	*** Input ***
18	diameter of conductor to fit in the slot (in)	dia'	from tables for AWG #4/0	0.29	*** Input ***
19	the corresponding area of conductor (in ²)	car	0.07	*** Input ***
20	area in circular mils	car	83690.00	*** Input ***
21	area in cm ²	car	42.41	*** Input ***
22	area in cm ²	car	0.42	
23	rotor bar resistivity (micro-ohms.cm)	sigma	from table for copper, B187	1.75	*** Input ***
24					
25					
26					
27					
28					
29					
30	peak current in loop u, amps	Iu	from program BDFM	300.00	*** Input ***
31 v	Iv	450.00	*** Input ***
32 w	Iw	600.00	*** Input ***
33 x	Ix	750.00	*** Input ***
34 y	Iy	900.00	*** Input ***
35					
36	rms current in loop u, amps	Iu	$I \cdot \text{peak} / \sqrt{2}$	212.13	rms

37	v	Iv	I-peak/sqrt(2)	318.20	rms
38	w	Iw	I-peak/sqrt(2)	424.26	rms
39	x	Ix	I-peak/sqrt(2)	530.33	rms
40	y	Iy	I-peak/sqrt(2)	636.40	rms
41	END-RING CURRENTS				
42					
43					
44	current in sub-section y, amps	Iy	Iy=Iy	636.40	
45	x	Iyx	Iyx=Iy+Ix	1166.73	
46	w	Iyxw	Iyxw=Iy+Ix+Iw	1590.99	
47	v	Iyxwv	Iyxwv=Iy+Ix+Iw+Iv	1909.19	
48	u	Iyxwvu	Iyxwvu=Iy+Ix+Iw+Iv+Iu	2121.32	
49					
50	rotor current density, amps/square inch	deltar	deltar=1.2*delta; .2 assumed	4500.00	*** Input ***
51					
52					
53	conductor area for loop u (ln^2)	cau'	cau'=Iu/deltar	0.05	calculated
54	conductor area for loop u (ln^2)	cau	selected	0.05	*** Input if different area than calculated one ***
55	conductor diameter / width (ln)	diau	selected	0.22	*** Input if different than square bar ***
56	current density in bar u (amp/ln^2)	deltau	deltau=Iu/cau	4500.00	
57					
58					
59	conductor area for loop v (ln^2)	cav'	cav'=Iv/deltar	0.07	calculated
60	conductor area for loop v (ln^2)	cav	selected	0.07	*** Input if different area than calculated one ***
61	conductor diameter / width (ln)	dIav	selected	0.27	*** Input if different than square bar ***
62	current density in bar v (amp/ln^2)	deltav	deltav=Iv/cav	4500.00	
63					
64					
65	conductor area for loop w (ln^2)	caw'	caw'=Iw/deltar	0.09	calculated
66	conductor area for loop w (ln^2)	caw	selected	0.09	*** Input if different area than calculated one ***
67	conductor diameter / width (ln)	dIaw	selected	0.31	*** Input if different than square bar ***
68	current density in bar w (amp/ln^2)	deltaw	deltaw=Iw/caw	4500.00	
69					
70					
71	conductor area for loop x (ln^2)	cax'	cax'=Ix/deltar	0.12	calculated
72	conductor area for loop x (ln^2)	cax	selected	0.12	*** Input if different area than calculated one ***
73	conductor diameter / width (ln)	dIax	selected	0.34	*** Input if different than square bar ***
74	current density in bar x (amp/ln^2)	deltax	deltax=Ix/cax	4500.00	
75					
76					
77	conductor area for loop y (ln^2)	cay'	cay'=Iy/deltar	0.14	calculated

78	conductor area for loop y (ln^2)	cay	selected	0.14	*** Input if different area than calculated one ***
79	conductor diameter / width (ln)	dlay	selected	0.38	*** Input if different than square bar ***
80	current density in bar y (amp/ln^2)	deltay	deltay=ly/cay	4500.00	
81					
82					
83	conductor area for end ring (ln^2)	cae'	cae'=lyxwv/deltar	0.47	assuming the same current density as in loops
84	conductor area selected (ln^2)	cae	selected	0.50	*** Input if different area than calculated one ***
85	end ring dimensions (ln)	w x l	w x l=.5 x l: copper plate	0.50	*** Input if different than square bar ***
86	(ln)			1.00	*** Input if different than square bar ***
87	current density in end ring bar (amp.ln^2)	deltac	deltac=lyxwv/cae	4242.64	
88					
89	ROTOR SLOT AND TOOTH WIDTH				
90					
91					
92					
93	rotor slot width for bar -u (ln)	wsru	wsru=diau+.03	0.25	.03 allowance for irregularity
94	rotor slot width for bar -v (ln)	wsrv	wsrv=dlav+.03	0.30	
95	rotor slot width for bar -w (ln)	wsrw	wsrw=dlaw+.03	0.34	
96	rotor slot width for bar -x (ln)	wsrx	wsrx=dlaux+.03	0.37	
97	rotor slot width for bar -y (ln)	wsry	wsry=dlay+.03	0.41	
98					
99	rotor teeth width (ln)	wtr	wtr=(pi*Dr-B*(wsru+wsrv+wsrw+wsrx+wsry))/40	0.84	assuming uniform teeth width
100					
101					
102	slot pitch for loop -u (ln)	lamdau	wsru+wtr	1.09	
103	slot pitch for loop -v (ln)	lamdv	lamdv=wsrv+2wsru+3wtr	3.32	
104	slot pitch for loop -w (ln)	lamdw	lamdw=wsrw+2wsrv+2*wsru+5wtr	5.63	
105	slot pitch for loop -x (ln)	lamdax	lamdax=wsrx+2wsrw+2wsrv+2*wsru+7wtr	8.03	
106	slot pitch for loop -y (ln)	lamday	lamday=wsry+2wsrx+2wsrw+2wsrv+2*wsru+9wtr	10.49	
107					
108	ROTOR SLOTS DEPTH				
109					
110					
111					
112					
113					
114	slot depth-u (ln)	dsu	dsu=diau+tt	0.25	tt- tooth thickness
115	slot depth-v (ln)	dsv	dsv=dlav+tt	0.30	
116	slot depth-w (ln)	dsw	dsw=dlaw+tt	0.34	
117	slot depth-x (ln)	dsx	dsx=dlaux+tt	0.37	
118	slot depth-y (ln)	dsy	dsy=dlay+tt	0.41	

119	rotor diameter at the botom of deepest slot-in	Drs	$Drs=Dr-2*dsy$	14.13	
120	shaft diameter (in)	Ds	from existing drive data sheet	3.38	*** Input***
121	core depth behind the deepest slot (in)	crdtr	$crdtr=(Drs-Ds)/2$	5.38	more than enough
122					
123	ROTOR FLUX PROFILE				
124					
125					
126	total flux crossing the air gap (maxwells)	pheetr	$pheet=phec6*p6+phec2*p2$	8.07E-06	flux per pole times # of poles from both windings
127	total teeth area (in^2)	At	$At=nr*ta*wtr$	299.68	
128	maximum tooth flux density (lines/in^2)	Btrmax	$Btrmax=sqrt(2) * pheet/At$	3.81E-04	compared to 115k lines per square inch
129					
130	core flux density (lines/in^2)	Bc	$Bc=pheetr/(2*crdtr*La)$	84288.12	compared to 115k lines per square inch
131					
132	ROTOR RESISTANCES				
133					
134					
135					
136	bar length loop -u (in)	blu	$blu=2*La+lmdau$	18.89	
137	-v (in)	blv	$blv=2*La+lmdav$	21.12	
138	-w (in)	blw	$blw=2*La+lmdaw$	23.43	
139	-x (in)	blx	$blx=2*La+lmdax$	25.83	
140	-y (in)	bly	$bly=2*La+lmday$	28.29	
141					
142	rotor bar resistivity (micro-ohms.in)	sigma'	$sigma'=sigma * 10^{(-6)} * (tu/25.4 \text{ cm})$	6.89E-08	
143	resistance loop -u (ohms)	ru	$re=blu*sigma'/(cau^2)$	5.86E-04	
144	-v (ohms)	rv	$re=blv*sigma'/(cav^2)$	2.91E-04	
145	-w (ohms)	rw	$re=blw*sigma'/(caw^2)$	1.82E-04	
146	-x (ohms)	rx	$re=blx*sigma'/(cax^2)$	1.28E-04	
147	-y (ohms)	ry	$re=bly*sigma'/(cay^2)$	9.75E-05	
148					
149	diamter at the mean of deepest slot (in)	Drm	$Drm=Dr-dlay$	14.57	
150	end ring length (in)	el	$el=pi*Drm$	45.77	
151	end ring resistance (ohms)	re	$re=el*sigma'/(w^2)$	6.31E-06	
152					
153	SUBSEGMENT RESISTANCES OF END-RING				
154					
155					
156					
157	sub-segment-u (ohms)	rsubu	$rsubu=lmdau*sigma'/(w^2)$	1.50E-07	correspond to current Iyxvu
158	sub-segment-v (ohms)	rsubv	$rsubv=(lmdav-lmdau)*sigma'/(w^2)$	3.07E-07	correspond to current Iyxv
159	sub-segment-w (ohms)	rsubw	$rsubw=(lmdaw-lmdav)*sigma'/(w^2)$	3.19E-07	correspond to current Iyxw

160	sub-segment-x (ohms)	rsubx	$rsubx=(lamdax-lamdaw)*sigma/(w*I)$	3.30E-07	correspond to current Ix
161	sub-segment-y (ohms)	rsuby	$rsuby=(lamday-lamdax)*sigma/(w*I)$	3.39E-07	correspond to current Iy
162					
163	ROTOR COPPER LOSSES				
164					
165					
166	losses in loop -u (watts)	clu	$clu=nst*Iu^2*ru$	1.05E+02	
167	-v (watts)	clv	$clv=nst*Iv^2*rv$	1.18E+02	
168	-w (watts)	clw	$clw=nst*Iw^2*rw$	1.31E+02	
169	-x (watts)	clx	$clx=nst*Ix^2*rx$	1.44E+02	
170	-y (watts)	cl y	$cl y=nst*Iy^2*ry$	1.58E+02	
171					
172	LOSSES OF END-RING SUB-SEGMENTS				
173					
174					
175	losses in subsegment -y (watts)	Iy	$Iy=nst*Iy^2*rsuby$	5.50E-01	
176	losses in subsegment -yx (watts)	Iyx	$Iyx=nst*Iyx^2*rsubx$	1.80E+00	
177	losses in subsegment -yxw (watts)	Iyxw	$Iyxw=nst*Iyxw^2*rsubw$	3.23E+00	
178	losses in subsegment -yxwv (watts)	Iyxwv	$Iyxwv=nst*Iyxwv^2*rsubv$	4.47E+00	
179	losses in subsegment -yxwvu (watts)	Iyxwvu	$Iyxwvu=nst*Iyxwvu^2*rsubu$	2.70E+00	
180					
181	TOTAL ROTOR COPPER LOSS				
182					
183					
184	total rotor copper loss (watts)	wir	$wir=total\ loop\ losses+end-ring\ losses$	668.77	
185					
186	IRON LOSSES				
187					
188					
189	# of core vents	vn	assumed	12.00	*** Input***
190	vent diameter (in)	vd	assumed	1.00	*** Input***
191	rotor core vents volume (in^3)	vv	$vv=vn*vd^2*La/4$	83.88	
192					
193	rotor teeth volume (in^3)	tv	$tv=w1*La*(3dsu+2dsv+2dsw+2dsx+dsy)^4$	94.70	
194					
195	rotor slots volume (in^3)	sv	$sv=8(wsrw^2+wsrv^2+wsrw^2+wsrx^2+wsry^2)La$	40.33	
196					
197	shaft volume (in^3)	shv	$shv=pi*Ds^2*La/4$	79.62	
198					
199	volume of core behind slots(in^3)	crv	$crv=pi*Dr^2*La/4-(vv+tv+sv+shv)$	1531.46	
200					

201	weight of iron in rotor teeth (lb)	mtr	$mtr = .28 \cdot tv$	26.51	
202	weight of iron rotor core (lb)	mcr	$mcr = .28 \cdot crv$	428.81	
203					
204	total iron volume (in ³)	iv	$iv = tv + crv$	1626.16	
205	total iron weight (lb)	mi	$mi = mtr + mcr$	455.32	
206	watts per pound for teeth USS-A1-36, 26 gage	wibr'	from graph @ $B_1 = 32k$ lines per square inch, $fr = 60$ -Hz	0.46	
207	watts per pound for core USS-A1-36, 26 gage	wibr'	from graph @ $B_c = 70k$ lines per square inch, $fr = 60$ -Hz	2.00	
208	watts per pound for teeth @ $fr = 15$ -Hz	wibr	$wibr = wibr' \cdot (15/60)^2$	0.03	
209	watts per pound for core @ $fr = 15$ -Hz	wibr	$wibr = wibr' \cdot (15/60)^2$	0.13	
210	rotor teeth loss, watts	wtri	$wtri = wibr \cdot mtr$	0.76	
211	rotor core loss, watts	wcri	$wcri = wibr \cdot mcr$	53.60	
212	total rotor iron loss, watts	wri	$wri = wtri + wcri$	54.36	
213	total rotor loss, watts	wir	$wir = wri + wcri$	723.14	
214					
215	total machine loss @ 900 rpm, watts	ml	$ml = w6 + wcu2 + wir$	4041.83	2-pole iron loss not included since DC applied
216	machine efficiency @ 900 rpm	esta	$esta = 60 \cdot 746 / (60 \cdot 746 + ml)$	0.92	

Appendix-XI; BDFM Practical Design Spreadsheet

BDFM DESIGN; 6-POLE WINDING					
Item	DESCRIPTION	sym	FORMULA	VALUE	REMARKS
1	machine rated horse power	Hp	required	80.00	*** Input***
2	design diameter at air-gap, inches	D	actual	14.25	*** Input***
3	design axial length, inches	la	*****	11.25	*** Input***
4	# of phases	m	3-phase	3.00	*** Input***
5	rms line voltage (volts)	Vl	Vl=460	460.00	*** Input***
6	frequency (Hz)	fs	fs=60Hz	60.00	*** Input***
7	synchronous speed (rpm)	N	rated	1200.00	*** Input***
8	# of poles	p	given; =120*fs/N	6.00	
9	full load power factor	pf	design parameter (objective at full load)	0.90	*** Input*** (typical value)
10	full load efficiency	η	*****	0.92	*** Input*** (typical value)
11	phase voltage (volts)	E	$Vl/\text{sqr}(3)$	265.58	
12	full load phase current (amps)	Ip	$746*Hp/(3*E*eta*pf)$	98.46	
13	total number of stator slots	ns	given	72.00	*** Input*** (stator lamination design)
14	number of slots per pole per phase	nspp	$nspp=ns/m*p$	4.00	
15	# of slots per pole	nsf	such that # of slots/pole/phase >=2	12.00	
16	# of slots per phase	nsph	$nsph=nspp*p$	24.00	
17	# of electrical degrees between slots	β	$beta=180*p/ns$	15.00	
18	***** in rad	β	$ln rad=beta(deg)*pi/180$	0.26	
19	distribution factor	fd	$fd=\sin(nspp*beta/2)/nspp*\sin(beta/2)$	0.96	
20	coil span in electrical degrees	gamma	obtained from winding schematics	150.00	*** Input***
21	coil pitch (pu)	cp	assumed for the design to be 5/6	0.83	*** Input***
22	pitch factor	fp	$fp=\sin(gamma/2)$; 2-for double layer winding	0.97	gamma converted to radian
23	winding factor	d	$d=fd*fp$	0.93	typical values between (.90 to .96)
24	elec. specific loading (amper-cond./in)	Q	from design curves (typical)	675.00	*** Input***
25	average air-gap density (lines/in ²)	Bg	$Bg=4.07*Hp*10^{-11}/(D^2*La*Q*d*N*eta*pf)$	2.30E+04	
26	DIMENSIONS ASSOCIATED WITH GIVEN SLOT				
27					
28	available slot depth	asd	given: including tooth thickness, wedge and curve	1.15	*** Input***
29	radius of curvature	rc	given	0.22	
30	tooth thickness	tt	fixed	0.83	
31	wedge thickness	wdt	fixed	0.05	
32	diameter at bottom of slot (excluding the arc)	Db	$Db=d+2*(asd-rc)$	16.12	
33	slot pitch at Db	lamdab	$lamdab=pi*Db/ns$	0.70	
34	slot width at Db	wsb	$wsb=lamdab-wt$	0.40	

36	tooth width at Db	wt	$wt = lamda b - 2 * rc$	0.30	this is uniform since parallel teeth are used
37	diameter at the mean depth of the slot	Dm	$Dm = D + 2 * bsd / 2$	15.40	
38	slot pitch at Dm	lamdam	$lamdam = pi * Dm / ns$	0.67	
39	the mean slot width	wsm	$wsm = lamdam - wt$	0.37	
40	diameter at narrow end of the slot	Dn	$Dn = D + 2 * (t + wdt)$	14.41	
41	slot pitch at the narrow end	lamdan	$lamdan = pi * Dn / ns$	0.63	
42	slot width at the narrow end Dn	wsn	$wsn = lamdan - wt$	0.33	
43	slot pitch at air-gap periphery	lamda	$lamda = pi * D / ns$	0.62	
44	pole pitch; designed (ln)	tau	$D * pi * cp / p$	6.22	design value used for calculations
45					
46	surface area at air-gap	sag	$sag = pi * D * La$	503.64	
47	teeth surface area at slot mean diameter	tsa	$tsa = w * La * ns$	245.58	
48	SLOT AND PHASE ORIGINAL # OF CONDUCTORS				
49					
50					
51	# of stator conductors per slot calculated	Cs'	$Cs' = Q * lamda / lp$	4.64	calculated at mean length
52 selected	Cs	# of cond/slot must be even # for dbl lyr wndng	4.00	*** Input*** (must be even)
53	# of stator conductors per phase	Z	$Z = Cs * nspp * p$	96.00	
54					
55	FLUX AND FLUX DENSITIES				
56					
57	air-gap flux per pole (lines "maxwells")	phi	$phce = E * 10^8 / (1.22 * d * f * Z)$	1.25E+06	
58	corrected air-gap density (lines/in^2)	Bg	$Bg = phce / tau * la$	32098.21	
59	maximum air gap density (lines/in^2)	Bgm	$Bgm = sqrt(2) * Bg$	45393.73	
60	maximum teeth density corrected, (lines/in^2)	Btm	$Btm = sag * Bgm / tsa$	93093.90	
61					
62	SELECTED CONDUCTORS				
63					
64	current density; assumed, (amp/in^2)	Delta	assumed; between (2000 - 3000) amps/in^2	4500.00	
65	cond. cross sectional area, calculated (in^2)	ca'	$ca' = lp / delta$	0.02010331	avg#6 area is .0206 in^2, .162 in dia
66	actual conductor diameter/thickness, (in)	dia	to fit the above calculated area	0.162	*** Input***
67"area, (in^2), (in)	ca	one awg#5 at .026 in^2	0.02061	*** Input***
68	substitute conductor area (in^2)	cas	one AWG#17 @ .001609	0.001609	*** Input***
69	substitute conductor diameter (in)	dias	one AWG#17 @ .04526	0.04526	*** Input***
70	# of stator substitute conductors per slot	Css'	$Css' = Cs * (ca / cas)$	51.236793	Css must be even for double layer winding
71	Css	chosen so that it is even and satisfies ca'	64	*** Input***
72	# of parallel conductors	pc	$pc = Css / Cs$	16	FLAG: integer parallel conductors OK
73	current density (amp/in^2)	delta	$delta = lp / (pc * cas)$	3514.02	FLAG: CURRENT DENSITY WITHIN RANGE
74	CHECK IF # OF SUBSTITUTE CONDUCTORS SATISFIES ca'			".....>	FLAG: CALCULATED AREA SATISFIED
75					
76					

77	CALCULATED SLOT DIMENSIONS FOR THE 6-POLE CONDUCTORS			
78				
79				
80	thickness of insulation (in)	ti	ti=15/1000	0.01 typical value, fixed
81	slot width available for wires, (in)	wsw	wsw=wsm-2*ti	0.34876733
82	number of cond. which can fit slot width	wnl	wnl=integer(wsw/dias)	7
83	# of rows of wires in the slot	wr	wr=csw/wnl	9.14285714
84	selected	wr	rounded to highest integer	10 *** Input ***
85	depth of wires stacked in the slot, (in)	wd	wd=wr*dias	0.4526
86	double layer spacer	dis	dis=30/1000 "	0.03 fixed
87	slot lining	ls	ls=insulation thickness	0.01 fixed
88	allowance for spaces between wires	all	all=3/1000"	0.03 fixed
89	slot depth of the 6-pole (in)	ds6	ds6=wd+dis+ls+all	0.5226
90				
91	DOUBLE LAYER WINDING CALCULATIONS			
92				
93	# of coils sides per slot	csps	csps=2; for double layer windings	2.00 *** Input ***
94	# of coil sides per phase	csph	csph=nsph*csps	48.00
95	# of coils per phase	cph	cph=csph/2	24.00 2-coil sides per coil
96	# of coil per pole per phase	cpph	cpph=cph/p	4.00
97	# of conductors per coil side	cpcs	cpcs=Cu/csph	2.00
98	# of turns per coil	Nc	Nc=cpcs	2.00
99	# of turns per phase in series	Ns	Ns=Nc*cph	48.00
100				
101	6-POLE RESISTANCE PER PHASE			
102				
103				
104	coil thickness plus clearance between end coils(in)	d1	d1=wsm+s	0.49 s was assumed to be .12
105	approximate angle of bend of end winding (rad)	alpha	alpha=arcsin(d1/lambdam)	0.81
106	pole pitch at the mean of the slot (in)	taum	taum=pi*(D+asd)*cp/P	6.72
107	end winding horizontal length of one end	2h	2h=taum/cos(alpha)	9.79
108	overhang length	oh	assumed to be the size of the slot depth	1.15
109	mean length per turn of stator winding	mlt	mlt=2*ls+.4*oh+2*(2h)	46.68
110	winding length per phase (ft)	wl	wl=Ns*mlt/12	186.74
111	resistance per M ft of specified conductor	rs'	from NEC @ 75 deg C	5.06 *** Input***
112	resistance per phase ohms	rs	rs=wl*rs'/(1000*pc)	0.06 resistance per 1000 ft given by AWG wire table
113				
114	6-POLE COPPER LOSSES			
115				
116	IR drop per phase (volts)	IR	IR=Ip*rs	5.35
117	total stator copper loss, 6-pole (Watts)	wcu6	wcu6=3*Ip*IR	1451.05

118					
119	6-POLE IRON LOSSES				
120					
121	core depth behind slots: 6-pole (in)	crd	measured	1.23	*** Input***
122	flux in stator core/pole (lines)	phec	assume to be half that of air gap	1.12E+06	
123	flux density in iron of stator lines/in ²	Bc	$Bc = phec / (in * crd)$	81460.49	
124	outside diameter, (in)	Do	$Do = 2 * (crd + asd) + D$	19.00	calculated
125					
126					
127					
128	weight of iron in stator core (lb)	mc	$mc = .28 * pi * (Do - crd) * crd * ln$	215.48	assuming .28lb/cubic in; for USS M-36
129	weight of iron in stator teeth (lb)	mt	$mt = .28 * wt * ds * ns * ln$	79.08	assuming uniform tooth width
130	watts per pound for core USS-M-36, 26 gage	wbc	obtained from graph @ Bc=82k lines/in ²	2.10	*** Input***
131	watts per pound per cycle for tooth	wbt @ Bt=78k lines/in ²	1.90	*** Input***
132	core loss	wcl	$wcl = wbc * mc$	452.51	
133	teeth loss	wtl	$wtl = wbt * mt$	150.25	
134	total stator iron loss (watts)	wsl6	$wsl6 = wcl + wtl$	602.75	
135	total stator loss (6-pole)	wl6	$wl6 = wcu6 + wsl6$	2053.80059	

BDFM DESIGN; 2-POLE WINDING					
Item	DESCRIPTION	sym	FORMULA	VALUE	REMARKS
1	machine rated horse power	Hp	required	120.00	*** Input***
2	DESIGN DIAMETER	D	actual	14.25	*** Input***
3	DESIGN LENGTH	la	11.25	*** Input***
4	# of phases	m	3-phase	3.00	*** Input***
5	rms line voltage (volts)	Vl	Vl=460	1300.00	*** Input***
6	frequency (Hz)	fs	fs=60Hz	-60.00	*** Input***
7	synchronous speed (rpm)	N	rated	-3600.00	*** Input***
8	# of poles	p	given; = 120°fs/N	2.00	*** Input***
9	full load power factor	pf	design parameter (objective at full load)	0.88	*** Input*** (typical values)
10	full load efficiency	η	0.90	*** Input*** (typical values)
11	phase voltage (volts)	E	$Vl/\sqrt{3}$	796.74	
12	full load phase current (amps)	Ip	$746 \cdot Hp \cdot \text{eta} / (3 \cdot E \cdot \text{pf})$	38.30	note the effect of efficiency compared to 6-pole
13	total number of stator slots	ns	given	72.00	*** Input***
14	number of slots per pole per phase	nspp	$nspp = ns/m \cdot p$	12.00	
15	# of slots per pole	nsp	such that # of slots/pole/phase >= 2	36.00	
16	# of slots per phase	nsph	$nsph = nspp \cdot p$	24.00	
17	# of electrical degrees between slots	β	$\text{beta} = 180 \cdot p / ns$	5.00	
18 in rad	β	$\text{In rad} = \text{beta}(\text{deg}) \cdot \pi / 180$	0.09	
19	distribution factor	fd	$fd = \sin(nspp \cdot \text{beta} / 2) / nspp \cdot \sin(\text{beta} / 2)$	0.96	
20	coil span in electrical degrees	gamma	obtained from winding schematics	150.00	*** Input***
21	coil pitch (pu)	cp	assumed for the design to be 5/6	0.83	*** Input***
22	pitch factor	fp	$fp = \sin(\text{gamma} / 2)$; 2-for double layer winding	0.97	gamma converted to radian
23	winding factor	d	$d = fd \cdot fp$	0.92	typical values between (.90 to .96)
24	elec. specific loading (amper-cond./in)	Q	from design curve (typical)	700.00	*** Input***
25	average air-gap density (lines/in²)	Bg	$Bg = 4.07 \cdot Hp \cdot 10^{-11} / (D^2 \cdot La \cdot Q \cdot d \cdot N \cdot \text{eta} \cdot \text{pf})$	-1.16E+04	
26					
27	DIMENSIONS ASSOCIATED WITH GIVEN SLOT				
28					
29	available slot depth	asd	given: including tooth thickness, wedge and curve	1.15	*** Input***
30	radius of curvature	rc	given	0.22	
31	tooth thickness	tt	fixed	0.03	
32	wedge thickness	wtd	fixed	0.05	
33	diameter at bottom of slot (excluding the arc)	Db	$Db = d + 2 \cdot (asd - rc)$	16.12	
34	slot pitch at Db	lamdab	$\text{lamdab} = \pi \cdot Db / ns$	0.70	
35	slot width at Db	wsb	$wsb = \text{lamdab} - wt$	0.40	

36	tooth width at Db	wt	$wt = \lambda m d a b - 2 * r c$	0.30	this is uniform since parallel teeth are used
37	diameter at the mean depth of the slot	Dm	$Dm = D + 2 * a s d / 2$	15.40	
38	slot pitch at Dm	lamdam	$lamdam = \pi * Dm / ns$	0.67	
39	the mean slot width	wsm	$wsm = lamdam - wt$	0.37	
40	diameter at narrow end of the slot	Dn	$Dn = D + 2 * (t + wdt)$	14.41	
41	slot pitch at the narrow end	lamdan	$lamdan = \pi * Dn / ns$	0.63	
42	slot width at the narrow end Dn	wsn	$wsn = lamdan - wt$	0.33	
43	slot pitch at air-gap periphery	lamda	$lamda = \pi * D / ns$	0.62	
44	pole pitch: designed (in)	τ	$D * \pi * cp / p$	18.65	design value used for calculations
45					
46	surface area at air-gap	sag	$sag = \pi * D * La$	503.64	
47	teeth surface area at slot mean diameter	tssa	$tssa = wt * La * ns$	245.58	
48	SLOT AND PHASE ORIGINAL # OF CONDUCTORS				
49					
50					
51	# of stator conductors per slot calculated	Cs'	$Cs' = Q * lamda / lp$	11.36	calculated at mean length
52 selected	Cs	# of cond/slot must be even # for dbl lyr wndng	10.00	*** Input***
53	# of stator conductors per phase	Z	$Z = Cs * nspp * p$	240.00	
54					
55	FLUX AND FLUX DENSITYIES				
56					
57	air-gap flux per pole (lines "maxwells")	ϕ	$phex = E * 10^8 / (2.22 * d * P * Z)$	-2.70E+06	
58	corrected air-gap density (lines/in^2)	Bg	$Bg = phex / tau * la$	-12871.94	
59	maximum air gap density (lines/in^2)	Bgm	$Bgm = sqrt(2) * Bg$	-18203.67	
60	maximum teeth density corrected, (lines/in^2)	Btm	$Btm = sag * Bgm / tsa$	-37332.27	
61					
62	SELECTED CONDUCTORS				
63					
64	current density; assumed, (amp/in^2)	Δ	assumed; between (2000 - 3000) amps/in^2	3700.00	
65	cond. cross sectional area, calculated (in^2)	ca'	$ca' = lp / delta$	0.010352339	awg#9 area is .0103 in^2, .1144 in dia
66	actual conductor diameter/thickness, (in)	dla	to fit the above calculated area	0.1144	*** Input***
67 area, (in^2), (in)	ca	one awg#5 at .026 in^2	0.01028	*** Input***
68	substitute conductor area (in^2)	cas	one AWG#17 @ .001609	0.001609	*** Input***
69	substitute conductor diameter (in)	dlaS	one AWG#17 @ .04526	0.04526	*** Input***
70	# of stator substitute conductors per slot	CsS'	$CsS' = Cs * (ca / cas)$	63.89061529	CsS must be even for double layer winding
71	CsS	chosen so that it is even and satisfies ca'	70	*** Input***
72	# of parallel conductors	pc	$pc = CsS / Cs$	7	FLAG: Integer parallel conductors OK
73	current density (amp/in^2)	delta	$delta = lp / (pc * cas)$	3400.84	FLAG: CURRENT DENSITY HIGH
74 CHECK IF # OF SUBSTITUTE CONDUCTORS SATISFIES ca'			".....->	FLAG: CALCULATED AREA SATISFIED
75					
76					

77	CALCULATED SLOT DIMENSIONS FOR THE 2-POLE CONDUCTORS			
78				
79				
80	thickness of insulation (in)	ti	ti=15/1000	0.01 typical value, fixed
81	slot width available for wires, (in)	wsw	wsw=wsm-2*ti	0.348767333
82	number of cond. which can fit slot width	wn1	wn1=integer(wsw/dias)	7
83	# of rows of wires in the slot	wr	wr=css/wn1	10
84 selected	wr	rounded to highest integer	10 *** Input ***
85	depth of wires stacked in the slot, (in)	wd	wd=wr*dias	0.4526
86	double layer spacer	dis	dis=30/1000 "	0.03 fixed
87	slot lining	ls	ls=insulation thickness	0.01 fixed
88	allowance for spaces between wires	all	all=3/1000"	0.03 fixed
89	slot depth of the 2-pole (in)	ds2	ds2=wd+dis+ls+all	0.5226
90				
91	DOUBLE LAYER WINDING CALCULATIONS			
92				
93	# of coils sides per slot	csps	csps=2; for double layer windings	2.00 *** Input ***
94	# of coil sides per phase	csph	csph=nsp*csps	48.00
95	# of coils per phase	cph	cph=csph/2	24.00 2-coil sides per coil
96	# of coil per pole per phase	cpph	cpph=cph/p	12.00
97	# of conductors per coil side	cpcs	cpcs=C/csp	5.00
98	# of turns per coil	Nc	Nc=cpcs	5.00
99	# of turns per phase	Ns	Ns=Nc*cph	120.00
100	2-POLE RESISTANCE PER PHASE			
101				
102				
103				
104	coil thickness plus clearance between end coils(in)	d1	d1=wsm+s	0.49 s was assumed to be .12
105	approximate angle of bend of end winding (rad)	alpha	alpha=arcsin(d1/lambdam)	0.81
106	pole pitch at the mean of the slot (in)	taum	taum=pi*(D+asd)*cp/P	20.16
107	end winding horizontal length of one end	2h	2h=taum/cos(alpha)	29.38
108	overhang length	oh	assumed to be the size of the slot depth	1.15
109	mean length per turn of stator winding	mlt	mlt=2*la+4*oh+2*(2h)	85.85
110	winding length per phase (ft)	wl	wl=Ns*mlt/12	858.52
111	resistance per M ft of specified conductor	rs'	from NEC @ 75 deg C	5.06 *** Input***
112	resistance per phase ohms	rs	rs=wl*rs'/(1000*pc)	0.62 resistance per 1000 ft given by AWG wire table
113				
114	2-POLE COPPER LOSSES			
115				
116	IR drop per phase (volts)	IR	IR=Ip*rs	23.79
117	total stator copper loss, 6-pole (Watts)	wcu2	Wcu6=3*Ip*IR	2733.67

118	2-POLE IRON LOSSES				
119					
120					
121	core depth behind slots: 6-pole (in)	crd	measured	1.23	*** Input***
122	flux in stator core/pole (lines)	ph _{ec}	assume to be half that of air gap	-1.35E+06	
123	flux density in iron of stator lines/in ²	B _c	B _c =ph _{ec} /(l _a *crd)	-98801.20	
124	outside diameter, (in)	D _o	D _o =2(crd+asd)+D	19.00	calculated
125					
126					
127					
128	weight of iron in stator core (lb)	m _c	m _c =.28*pi*(D _o -crd)*crd*l _a	215.48	assuming .28lb/cubic in; for USS M-36
129	weight of iron in stator teeth (lb)	m _t	m _t =.28*wt*ds*ns*l _a	79.08	assuming uniform tooth width
130	watts per pound for core USS-M-36, 26 gage	w _{bc} '	from graph @ B _c =98k, f _c =60-Hz lines/in ²	3.30	*** Input***
131	watts per pound per cycle for tooth	w _{bt} '	***** @ B _t = 32k, f _c =60-Hz lines/in ²	0.40	*** Input***
132	watts per pound for core @ f _c =20-Hz	w _{bc}	w _{bc} =w _{bc} '*(20/60) ²	0.37	
133	watts per pound for teeth @ f _c =20-Hz	w _{bt}	w _{bt} =w _{bt} '*(20/60) ²	0.04	
134	core loss	w _c	w _c =w _{bc} *m _c	79.01	
135	teeth loss	w _t	w _t =w _{bt} *m _t	3.51	
136	total stator iron loss (watts)	w _{st} 2	w _{st} 2=w _c +w _t	82.52	
137	total stator loss (2-pole)	w _l 2	w _l 2=w _c 2+w _{st} 2	2816.198842	

COMMON CALCULATIONS FOR BOTH WINDINGS					
Item	description	sym	formula	value	remark
1					
2	TOTAL STATOR LOSSES				
3					
4	total stator copper loss (watts)	wcu1	$wcu1 = wcu16 + wcu2$	4184.72	
5	total stator iron loss (watts) @ rated speed	wsl1	$wsl1 = wsl16$	482.75	2-pole winding has DC excitation @ 900-rpm
6	total stator loss (watts)	wsl	$wsl = wcu1 + wsl1$	4787.47	
7					
8	MAX. INSTANTANEOUS TEETH FLUX DENSITY				
9					
10					
11					
12					
13	maximum instantaneous flux density	Btm	$Btm = Btm6 + Btm2 $	130426.1616	FLAG; HIGH TEETH FLUX DENSITY
14	maximum instantaneous core flux density	Bcm	$Bcm = Bc6 + Bc2 $	179461.6938	FLAG; HIGH CORE FLUX DENSITY
15					
16					
17	CALCULATED SLOT DEPTH AND CONDUCTORS AREA				
18					
19					
20					
21	wedge thickness (in)	wdt	$wdt = 30/1000''$	0.0483	***Input***
22	tooth thickness (in)	tt	assumed	0.03	***Input***
23	spacer between the two windings (in)	s62	may not be required	0.03	***Input***
24	total slot depth, (in)	ds	$ds = ds6 + ds2 + wdt + tt$	1.1535	FLAG; INSUFFICIENT SLOT DEPTH
25					
26	total # of conductors in the slot	c	$c = Cas6 + Cas2$	134	
27	area of conductors	cas	from the 2/6-pole designs	0.001609	
28	total area required by all conductors in the slot	cat	$cat = cas * c$	0.215606	Flag: slot area adequate for specified # of conductors
29					
30	ACTUAL SLOT AREA CALCULATION				
31					
32					
33					
34	equivalent slot width	esw	$esw = wsn + (wsb - wsn)/2$	0.362711041	
35	slot depth excluding the arc and area below wedge	eqd	$eqd = dsd - wdt - tt - rc$	0.8546	
36	actual slot area available for wires	saaw	$saaw = eqd * esw * pi * rc^2 / 2$	0.309972855	

37	fill factor	ff	assumed	0.71	*** Input***
38	fillable area	fa	fa=ff*saaw	0.220080727	
39					
40	SUMMARY SHEET				
41					
42					
43					
44			6-POLE WINDING		
45					
46					
47					
48	type of winding used		double layer winding		
49	wire size used		# 17 AWG		
50	fractional pitch	fp	assumed for this design	0.83	5/6 th fractional pitch used
51	total number of conductors used/slot	Css6		64	
52	number of parallel conductors	pc6		16	
53	number of coils per pole per phase	cpph		4	
54	number of turns per coil	Nc		2	
55	number of turns/phase	Ns6		48	
56					
57			2-POLE WINDING		
58					
59					
60	type of winding used		double layer winding		
61	wire size used		# 17 AWG		
62	fractional pitch	fp	assumed	0.83	5/6 th fractional pitch used
63	total number of conductors used/slot	Css2		70	
64	number of parallel conductors	pc2		7	
65	number of coils per pole per phase	cpph		12	
66	number of turns per coil	Nc		5	
67	number of turns	NS2		120	
68					
69					
70	DESIGN DIAMETER (in), (m)	D	(in), (m)	14.25	0.36195
71	DESIGN LENGTH (in), (m)	la	(in), (m)	11.25	0.28575
72	DESIGN AIR-GAP LENGTH (in), (m)	Lg	$Lg = 125 - (10.17 / (D + 90))$	0.03	0.000697129
73	DESIGN AIR-GAP LENGTH (mm)			0.70	
74					
75					
76					
77					

BDFM ROTOR DESIGN					
Item	description	sym	formula	value	remark
1					
2	number of rotor poles	pr	constant for bdfm	4.00	*** Input ***
3	air-gap radial length (in)	lg	$lg = 125 \cdot (10.17/D + 90)$	0.03	
4	rotor diameter (in)	Dr	$Dr = D - 2 \cdot lg$	14.20	
5	number of rotor slots	nr	chosen to avoid cogging, cusping & noise	40.00	*** Input ***
6	number of nests	nst	known for BDFM	4.00	*** Input ***
7	number of slots per pole	nrp	$nrp = nr/pr$	10.00	
8	rotor slot pitch in degrees	lamdar'	$lamdar' = 360/nr$	9.00	
9	rotor slot pitch (in)	lamdar	$lamdar = lamdar' \cdot \pi \cdot Dr / 360$	1.11	
10	pole pitch (in)	taur	$taur = \pi \cdot Dr / pr$	11.15	
11					
12	ASSUMED ROTOR SLOTS DIMENSIONS AND ROTOR BARS CHARACTERISTICS USED TO CALCULATE BAR CURRENTS				
13					
14					
15					
16					
17	rotor slot width (in)	wsr'	assume a size to fit AWG #1 diameter	0.30	*** Input ***
18	diameter of conductor to fit in the slot (in)	dla'	from tables for AWG#4/0	0.29	*** Input ***
19	the corresponding area of conductor (in ²)	car	0.07	*** Input ***
20	area in circular mills	car	83690.00	*** Input ***
21	area in mm ²	car	42.41	*** Input ***
22	area in cm ²	car	0.42	
23	rotor bar resistivity (micro-ohms.cm)	sigma	from table for copper, B187	1.75	*** Input ***
24					
25	CALCULATED CURRENTS FROM BDFM SIMULATION PROGRAM				
26					
27					
28					
29					
30	peak current in loop u, amps	Iu	from program BDFM	300.00	*** Input ***
31 v	Iv	450.00	*** Input ***
32 w	Iw	600.00	*** Input ***
33 x	Ix	750.00	*** Input ***
34 y	Iy	900.00	*** Input ***
35					
36	rms current in loop u, amps	Iu	$I \cdot peak / \sqrt{2}$	212.13	rms

37	v	Iv	I-peak/sqrt(2)	318.20	rms
38	w	Iw	I-peak/sqrt(2)	424.26	rms
39	x	Ix	I-peak/sqrt(2)	530.33	rms
40	y	Iy	I-peak/sqrt(2)	636.40	rms
41	END-RING CURRENTS				
42					
43					
44	current in sub-section y, amps	Iy	Iy=Iy	636.40	
45	x	Iyx	Iyx=Iy+Ix	1166.73	
46	w	Iyxw	Iyxw=Iy+Ix+Iw	1590.99	
47	v	Iyxwv	Iyxwv=Iy+Ix+Iw+Iv	1989.19	
48	u	Iyxwvu	Iyxwvu=Iy+Ix+Iw+Iv+Iu	2121.32	
49					
50	rotor current density, amps/square inch	deltar	deltar=1.2*delta; .2 assumed	4500.00	*** Input ***
51					
52					
53	conductor area for loop u (in^2)	cau'	cau'=Iu/deltar	0.05	calculated
54	conductor area for loop u (in^2)	cau	selected	0.05	*** Input if different area than calculated one ***
55	conductor diameter / width (in)	diau	selected	0.22	*** Input if different than square bar ***
56	current density in bar u (amp/in^2)	deltau	deltau=Iu/cau	4500.00	
57					
58					
59	conductor area for loop v (in^2)	cav'	cav'=Iv/deltar	0.07	calculated
60	conductor area for loop v (in^2)	cav	selected	0.07	*** Input if different area than calculated one ***
61	conductor diameter / width (in)	dIav	selected	0.27	*** Input if different than square bar ***
62	current density in bar v (amp/in^2)	deltav	deltav=Iv/cav	4500.00	
63					
64					
65	conductor area for loop w (in^2)	caw'	caw'=Iw/deltar	0.09	calculated
66	conductor area for loop w (in^2)	caw	selected	0.09	*** Input if different area than calculated one ***
67	conductor diameter / width (in)	dIaw	selected	0.31	*** Input if different than square bar ***
68	current density in bar w (amp/in^2)	deltaw	deltaw=Iw/caw	4500.00	
69					
70					
71	conductor area for loop x (in^2)	cax'	cax'=Ix/deltar	0.12	calculated
72	conductor area for loop x (in^2)	cax	selected	0.12	*** Input if different area than calculated one ***
73	conductor diameter / width (in)	dIax	selected	0.34	*** Input if different than square bar ***
74	current density in bar x (amp/in^2)	deltax	deltax=Ix/cax	4500.00	
75					
76					
77	conductor area for loop y (in^2)	cay'	cay'=Iy/deltar	0.14	calculated

78	conductor area for loop y (in ²)	ca _y	selected	0.14	*** input if different area than calculated one ***
79	conductor diameter / width (in)	d _{lay}	selected	0.38	*** input if different than square bar ***
80	current density in bar y (amp/in ²)	d _{elay}	d _{elay} =I _y /ca _y	4500.00	
81					
82					
83	conductor area for end ring (in ²)	cae'	cae'=lyxwv/d _{elay}	0.47	assuming the same current density as in loops
84	conductor area selected (in ²)	cae	selected	0.50	*** input if different area than calculated one ***
85	end ring dimensions (in)	w x l	w x l=.5 x l: copper plate	0.50	*** input if different than square bar ***
86	(in)			1.00	*** input if different than square bar ***
87	current density in end ring bar (amp.in ²)	d _{etae}	d _{etae} =I _y xwv/cae	4242.64	
88					
89					
90	ROTOR SLOT AND TOOTH WIDTH				
91					
92					
93	rotor slot width for bar -u (in)	ws _{ru}	ws _{ru} =d _{lau} +.03	0.25	.03 allowance for irregularity
94	rotor slot width for bar -v (in)	ws _{rv}	ws _{rv} =d _{lav} +.03	0.30	
95	rotor slot width for bar -w (in)	ws _{rw}	ws _{rw} =d _{law} +.03	0.34	
96	rotor slot width for bar -x (in)	ws _{rx}	ws _{rx} =d _{lax} +.03	0.37	
97	rotor slot width for bar -y (in)	ws _{ry}	ws _{ry} =d _{lay} +.03	0.41	
98					
99	rotor teeth width (in)	w _{tr}	w _{tr} =(π*Dr-S*(ws _{ru} +ws _{rv} +ws _{rw} +ws _{rx} +ws _{ry}))/40	0.78	assuming uniform teeth width
100					
101					
102	slot pitch for loop -u (in)	l _{amdu}	l _{amdu} =ws _{ru} +w _{tr}	1.03	
103	slot pitch for loop -v (in)	l _{amd_v}	l _{amd_v} =ws _{rv} +2ws _{ru} +3w _{tr}	3.14	
104	slot pitch for loop -w (in)	l _{amd_w}	l _{amd_w} =ws _{rw} +2ws _{rv} +2*ws _{ru} +5w _{tr}	5.34	
105	slot pitch for loop -x (in)	l _{amd_x}	l _{amd_x} =ws _{rx} +2ws _{rw} +2ws _{rv} +2*ws _{ru} +7w _{tr}	7.61	
106	slot pitch for loop -y (in)	l _{amd_y}	l _{amd_y} =ws _{ry} +2ws _{rx} +2ws _{rw} +2ws _{rv} +2*ws _{ru} +9w _{tr}	9.96	
107					
108					
109					
110	ROTOR SLOTS DEPTH				
111					
112					
113					
114	slot depth-u (in)	d _{su}	d _{su} =d _{lau} +t _t	0.25	t _t - tooth thickness
115	slot depth-v (in)	d _{sv}	d _{sv} =d _{lav} +t _t	0.30	
116	slot depth-w (in)	d _{sw}	d _{sw} =d _{law} +t _t	0.34	
117	slot depth-x (in)	d _{sx}	d _{sx} =d _{lax} +t _t	0.37	
118	slot depth-y (in)	d _{sy}	d _{sy} =d _{lay} +t _t	0.41	

119	rotor diameter at the botom of deepest slot (in)	Drs	$Drs = Dr - 2 \cdot dsy$	13.38	
120	shaft diameter (in)	Ds	from existing drive data sheet	3.00	*** Input***
121	core depth behind the deepest slot (in)	crdtr	$crdtr = (Drs - Ds) / 2$	5.19	more than enough
122					
123	ROTOR FLUX PROFILE				
124					
125					
126	total flux crossing the air gap (maxwells)	pheetr	$pheetr = phec6 \cdot p6 \cdot phec2 \cdot p2$	8.07E+06	flux per pole times # of poles from both windings
127	total teeth area (in ²)	At	$At = nr \cdot la \cdot wir$	352.35	
128	maximum tooth flux density (lines/in ²)	Birmax	$Birmax = \sqrt{2} \cdot pheetr / At$	3.24E+04	compared to 115k lines per square inch
129					
130	core flux density (lines/in ²)	Bc	$Bc = pheetr / (2 \cdot crdtr \cdot La)$	69000.63	compared to 115k lines per square inch
131					
132	ROTOR RESISTANCES				
133					
134					
135					
136	bar length loop -u (in)	blu	$blu = 2 \cdot La + lamdau$	23.53	
137	-v (in)	blv	$blv = 2 \cdot La + lamdav$	25.64	
138	-w (in)	blw	$blw = 2 \cdot La + lamdaw$	27.84	
139	-x (in)	blx	$blx = 2 \cdot La + lamdax$	30.11	
140	-y (in)	bly	$bly = 2 \cdot La + lamday$	32.46	
141					
142	rotor bar resistivity (micro-ohms.in)	sigma'	$\sigma' = \sigma \cdot 10^{-6} \cdot (in/25.4 \text{ cm})$	6.89E-08	
143	resistance loop -u (ohms)	ru	$re = blu \cdot \sigma' / (cau^2)$	7.30E-04	
144	-v (ohms)	rv	$re = blv \cdot \sigma' / (cav^2)$	3.53E-04	
145	-w (ohms)	rw	$re = blw \cdot \sigma' / (caw^2)$	2.16E-04	
146	-x (ohms)	rx	$re = blx \cdot \sigma' / (cax^2)$	1.49E-04	
147	-y (ohms)	ry	$re = bly \cdot \sigma' / (cay^2)$	1.12E-04	
148					
149	diamter at the mean of deepest slot (in)	Drm	$Drm = Dr - diay$	13.82	
150	end ring length (in)	el	$el = \pi \cdot Drm$	43.41	
151	end ring resistance (ohms)	re	$re = el \cdot \sigma' / (w^2)$	5.98E-06	
152					
153					
154	SUBSEGMENT RESISTANCES OF END-RING				
155					
156					
157	sub-segment-u (ohms)	rsubu	$rsubu = lamdau \cdot \sigma' / (w^2)$	1.42E-07	correspond to current lyxwv
158	sub-segment-v (ohms)	rsubv	$rsubv = (lamdav - lamdau) \cdot \sigma' / (w^2)$	2.91E-07	correspond to current lyxw
159	sub-segment-w (ohms)	rsubw	$rsubw = (lamdav - lamday) \cdot \sigma' / (w^2)$	3.03E-07	correspond to current lyxw

160	sub-segment-x (ohms)	rsubx	$rsubx=(lamdax-lamdaw)*sigma/(w*l)$	3.14E-07	correspond to current Iyx
161	sub-segment-y (ohms)	rsuby	$rsuby=(lamday-lamdax)*sigma/(w*l)$	3.23E-07	correspond to current Iy
162					
163					
164	ROTOR COPPER LOSSES				
165					
166	losses in loop -u (watts)	clu	$clu=nst*lu^2*ru$	1.31E+02	
167	-v (watts)	clv	$clv=nst*lv^2*rv$	1.43E+02	
168	-w (watts)	clw	$clw=nst*lw^2*rw$	1.55E+02	
169	-x (watts)	clx	$clx=nst*lx^2*rx$	1.68E+02	
170	-y (watts)	cl y	$cl y=nst*ly^2*ry$	1.81E+02	
171					
172	LOSSES OF END-RING SUB-SEGMENTS				
173					
174					
175	losses in subsegment -y (watts)	ly	$ly=nst*ly^2*rsuby$	5.24E-01	
176	losses in subsegment -yx (watts)	lyx	$lyx=nst*Iyx^2*rsubx$	1.71E+00	
177	losses in subsegment -yxw (watts)	lyxw	$lyxw=nst*Iyxw^2*rsubw$	3.07E+00	
178	losses in subsegment -yxwv (watts)	lyxwv	$lyxwv=nst*Iyxwv^2*rsubv$	4.24E+00	
179	losses in subsegment -yxwvu (watts)	lyxwvu	$lyxwvu=nst*Iyxwvu^2*rsubv$	2.56E+00	
180					
181	TOTAL ROTOR COPPER LOSS				
182					
183					
184	total rotor copper loss (watts)	wir	$wir=total\ loop\ losses+end-ring\ losses$	791.06	
185					
186					
187	IRON LOSSES				
188					
189	# of core vents	vn	assumed	12.00	*** input***
190	vent diameter (in)	vd	assumed	1.00	*** input***
191	rotor core vents volume (in^3)	vv	$vv=vn*vd^3*La/4$	106.03	
192					
193	rotor teeth volume (in^3)	tv	$tv=wt^3*La*(3dsu+2dsv+2dsw+2dsx+dsy)^3/4$	111.34	
194					
195	rotor slots volume (in^3)	sv	$sv=B(wsrw^3+wsrv^3+wsrw^2+wsrx^2+wsry^2)*La$	50.98	
196					
197	shaft volume (in^3)	shv	$shv=pl^3*Ds^3*La/4$	79.52	
198					
199	volume of core behind slots (in^3)	crv	$crv=pl^3*Dr^3*La/4-(vv+tv+sv+shv)$	1734.74	
200					

